Lehigh University
Lehigh Preserve

Theses and Dissertations

1-1-1982

Growth and properties of niobium bicrystals.

Bing-Chu Cai

Follow this and additional works at: http://preserve.lehigh.edu/etd

Part of the Materials Science and Engineering Commons

Recommended Citation

Cai, Bing-Chu, "Growth and properties of niobium bicrystals." (1982). *Theses and Dissertations*. Paper 1961.

GROWTH AND PROPERTIES OF NIOBIUM BICRYSTALS

by

BING-CHU CAI

A Thesis

presented to the Graduate Committee

of Lehigh University

in Candidacy for the Degree of

Master of Science

in

Metallurgy and Materials Engineering

Lehigh University

1982

ProQuest Number: EP76234

ProQuest EP76234

CERTIFICATE OF APPROVAL

This thesis is accepted in partial fulfillment of the requirements for the degree of Master of Science.

May 5, 1982
(date)

Professor in Charge

Department Chairman

Table of Contents

Table of Contents (continued)

Acknowledgment

Abstract

A "match-up" seed method of growing bicrystals of niobium was developed. Experimental results show that the new method eliminates some of the limitations of the Y-shaped seed method previously reported.

Etch pits on various crystallographic planes of single crystals and bicrystals were observed. A relationship between the shape of the pits and the orientation of the etching surface was established and discussed on the basis of the surface energy concept.

Grain boundary hardening was determined by microhardness measurements. Boundary hardening was found to be misorientation dependent and related to the boundary energy. For bicrystals with low angle boundaries, boundary hardening varies with misorientation in a linear relationship of the Read-Shockley type. For bicrystals with high angle boundaries, hardening cusps (minima) were observed near the coincidence site lattice boundaries.

I. Introduction

The study of grain boundaries has received increasing attention as a subject of research because of their importance in the general field of physical metallurgy (phase transformation, diffusion, solidification, recrystallization, grain growth, etc.). The presence of grain boundaries often controls the occurrence of individual slip, twinning and cracking and hence has influence on deformation behavior and consequently mechanical properties. Grain boundary segregation of impurities is believed to be responsible for a variety of failure processes such as embrittlement, stress corrosion cracking, or cavitation.

In view of the significant effects of grain boundaries, the emphasis in the study of materials properties during the past decade has moved from the interior of grains to the interface of grains. The structure, energy, diffusion, sliding and migration of grain boundaries have been studied extensively. Successful applications of new techniques including transmission electron microscopy, computer simulation, field-ion microscopy and Auger spectroscopy, have greatly facilitated the direct examination or determination of the structure of grain boundaries.

Despite these recent developments, many problems, especially those involving the structures of grain boundaries, remain to be solved. Most previous studies of grain boundaries, however, were concerned with f.c.c. metals. Because of the difficulty in specimen preparations, boundary properties of b.c.c. metals, except for Fe-Si alloys, are practically unknown. The purpose of this investigation was to develop methods for growing bicrystals of b.c.c. metals with precontrolled orientation (niobium bicrystals, for example) and to provide new data on

-2-

grain boundary properties of these bicrystals. The present work, there-
fore, contains three separate parts: (a) methods of bicrystal growth,
(b) observation of etch pits and (c) measurements of grain boundary
hardening.
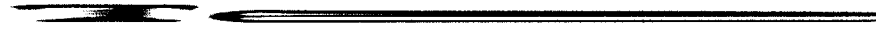
A New ============ chnique for the Growth of Bicrystals of Refractory Metals

1. Introduction

Pande, et al. [1,2] reported a method of growing bicrystals of refractory metals. The method utilized a special seeding procedure in which a single crystal seed was first grown from a polycrystalline rod in a vertical floating-zone electron beam melting unit. The top end of the resultant single crystal was cut along a center plane, thereby yielding two split sections which were then bent apart symmetrically with respect to the center plane of the crystal. This Y-shaped crystal was used as a bicrystal seed that could grow into a polycrystalline rod placed above it. A schematic representation is shown in Fig. 1.

Although the Y-shaped seed method has been used successfully in the growth of symmetrical tilt boundary bicrystals, it has certain limitations. The bicrystal metal must be ductile. Thus it is not suitable for hard metals such as Mo, W, or Cr. In addition, the method is not effective for bicrystals with large-angle boundaries, and it is not applicable for nonsymmetrical bicrystals.

Recent studies [3] on grain-boundary flux pinning in niobium super-conductors have indicated the importance of obtaining nonsymetrical bicrystal samples with high angle boundaries. In an effort to provide such samples, a modification of the Y-shaped seed method that overcomes some of the short-comings mentioned above was developed. The modified growth process is reported in this note.

2. Preparation of a Bicrystal Seed

In one of our early attempts in niobium bicrystal growth, the bi-crystal seeds were made from two half cylinders, each cut from a single crystal rod of preassigned orientation. The two half crystals were placed face to face and tied together with a fine niobium wire. The "match up" seed was then used for bicrystal growth. Unfortunately, none of these trials succeeded. It was learned, during later development of the Y-shaped seed method, that the failure was due to uneven heat flow in the two sections of the bicrystal seed. It appears that continuous, uniform heat flow is necessary for successful growth. This important feature is taken into account in the present approach to bicrystal growth.

The new approach may be illustrated conveniently by a special bicrystal growth procedure for the study of flux pinning in niobium bicrystals [3]. The theory of Campbell and Evetts for flux pinning by grain boundaries [4] emphasizes the anisotropy of H_{C2} in the material. In niobium, the highest and lowest H_{C2} are known to be along the $<111>$ and $<100>$ directions, respectively. For the maximum difference in H_{C2} between these two directions, a maximum elementary pinning force is expected. To verify this theory, it is desirable to measure the pinning force on a niobium bicrystal in which one crystal is parallel to the $<111>$ and the other to the $<100>$ direction (Fig. 2). Such a bicrystal sample was prepared by the following procedure (see Fig. 3).

Two single crystals with [011] orientation, in the shape of a rod 0.635 cm in diameter and at least 4 cm in length, were grown in a vertical floating-zone electron beam melting unit. One rod was cut longitudinally along the $(2\bar{1}1)$ plane (step i), and the other along the $(0\bar{1}1)$ plane (step ii).

-6-

One half was selected from each rod, and the two halves were placed together to form a composite unit, which was tied together with a fine niobium wire. A large section of the unit was then remelted in the electron beam melting unit. However, a portion 12 mm long at one end of the composite (the end which would ultimately serve as the bicrystal seed) was not exposed to the electron beam and, therefore, remained unmelted (steps iii and iv). This seed was then used for growing the bicrystal with a controlled asymmetrical tilt grain boundary. The remelting of a major portion of the composite unit alleviated the problem of uneven heat flow in the bicrystal seed. The long cut down the axis of each rod and the remelting process made this procedure somewhat laborious. Consequently, a modification was made to simplify the process.

A [011] single crystal rod 5 cm in length was grown. This rod was cut into two halves at a depth of 12 mm along the (2$\bar{1}$1) plane in the longitudinal direction. These two half sections were then cut off the stem (Fig. 4, step i). The remaining portion of the single crystal was again cut in half at a depth of 12 mm, but this time along the (0$\bar{1}$1) plane (step ii). One half of the newly sectioned region was removed (step iii), and in its place was inserted one of the halves from the previous cut along the (2$\bar{1}$1) plane. The two halves were tied together with niobium wire (step iv).

It was evident, however, that the seed so prepared was not suitable for growing a bicrystal. The half crystal from the first cut had a much higher resistance to heat flow compared with the one that is contiguous with the stem, due to the gap existing in the path of its heat flow. Therefore, a local melting of this gap was necessary to assure that both crystals of the seed had the same conditions of heat conduction. This was

-7-

achieved by placing the heating filament around the gap. When the gap was welded, the power supply was reduced immediately (step v in Fig. 4). The filament was then moved to the end of the seed, and the bicrystal growth could begin. The key points in this method are that there must be a good fit between the two half crystals, and that the local melting of the gap must be over the entire cross section of the rod.

The above modified method is as effective as the original, but eliminates the necessity of a long cut and remelting. It was used successfully in our laboratory for the preparation of bicrystal seeds.

For the growth of bicrystals with symmetrical tilt grain boundaries, the procedure for seed preparation is similar to the above with a minor revision. Here the original single crystal seed is grown with the [011] direction deviated from the longitudinal axis by $\theta/2$ where θ is the desired misorientation angle. The planes cut along the two longitudinal sections are identical, and before the two crystals are matched together, the half cylinder from the first cut section is rotated through an angle of 180° to meet the symmetry of the tilt boundary. This sequence of seed preparation is illustrated in Fig. 5.

One may, in principle, simplify the above procedure by eliminating the step of the horizontal cut at the middle of the split cylinder (see Fig. 5). In this case, the right half of the split cylinder is initially removed, but then set back into its original position after a 180° rotation about the normal of the longitudinal

axis. The length of the center-plane sectioning can also be
reduced by one half. However, the drawback to this simplified
method is that the cross section of the seed part is slightly
different from that of the stem due to the removal of the material
by cutting. This would cause uneven heat flow in the growth pro-
cess, which is critical for bicrystal rods of small diameters.

In addition to niobium bicrystals, bicrystals of molybdenum
and chromium, which could not be produced by the Y-shaped seed
method because of their low ductility, have been grown successfully
using the present technique.

3. Discussion

The probability of success in bicrystal growth is affected by
a number of factors. One of these is the alignment of the seed and
the polycrystal charge in the electron beam melting unit, because
the symmetry of the temperature field in both crystals of the seed
depends upon the positions of the crystals inside the electron beam
filament. The shape of the filament is also important in order to
provide a uniform heat input. The control of the power supply which
induces a steep temperature gradient along the axial direction is
likewise critical. The correct power selection is achieved by con-
trolling the "neck" shape of the melting zone, and the speed control
of the filament must be matched with the power supply.

The above procedure for preparing symmetrical bicrystals with
tilt boundaries is to some extent similar to that used by Cheng and
Chou in their study of the fracture of molybdenum bicrystals [5].
Their method is shown schematically in Fig. 6 (for bicrystals with
tilt boundaries) and Fig. 7 (with twist boundaries). The main dif-

ference between the two methods is that in the previous approaches (including those of the diffusion bonding and arc zone-melting [6, 7]), the grain boundary is formed by a joining process and therefore is not a growth product, whereas in the present method the boundary grows continuously from its seed as the melting zone advances.

The present method can also be used for bicrystals with twist boundaries [5,8]. In this case, two single crystals of different orientations but with center planes having the same Miller indices are required. After sectioning along the center planes and matching the appropriate halves, the orientations of the two crystals at the interface differ by a preassigned angle. This yields a bicrystal seed of a known twist boundary.

In conclusion, the modified "match-up" seed method can be used for bicrystals of arbitrary misorientations and is suitable for both ductile and brittle metals. The probability of success is high for bicrystals with low grain boundary energies. For bicrystals with high grain boundary energies, the probability of success is satis-factory, but the length of the boundary would be somewhat shortened.

References

1. C. S. Pande, L. S. Lin, S. R. Butler and Y. T. Chou, J. Crystal Growth 19 (1973) 209.

2. C. S. Pande and Y. T. Chou, Treatise on Materials Science and Technology, vol. 8 (1975) 43.

3. A. DasGupta, C. C. Koch, D. M. Kroeger, and Y. T. Chou, Phil. Mag. 38B (1978) 367 ; Adv. Cryogen. Engng. 24 (1978) 350.

4. A. M. Campbell and J. E. Evetts, Adv. Phys. 21 (1972) 199.

5. F. L. Cheng and Y. T. Chou, Research Report, Department of Metallurgy and Materials Engineering, Lehigh University, 1974.

6. M. R. Achter, Naval Research Laboratory, Research Report No. 1718 (1966).

7. W. F. Brehm, Jr. and J. L. Gregg, J. Less-Common Met. 14 (1968) 465.

8. S. P. Clough, S. J. Vonk and D. F. Stein, J. Less-Common Met. 50 (1976) 161.

Fig. 1: Schematic diagram illustrating the Y-shaped seed method for growing ductile bicrystals: (i) single crystal grown on a polycrystalline rod; (ii) a longitudinal cut along a center plane; (iii) bending to form a Y-shaped bicrystal seed; (iv) alignment of polycrystalline charge; and (v) a bicrystal grown from its seed. (Pande, et al . [1].)

Fig. 2: A nonsymmetrical bicrystal.

Fig. 3: Schematic diagram illustrating the "match-up" seed method for bicrystal growth: (i) $(2\bar{1}\bar{1})$ cut; (ii) $(0\bar{1}1)$ cut; (iii) matching of two half crystals; and (iv) lower section remelted for even heat conduction.

Fig. 4: Schematic diagram showing the modified "match-up" seed method for bicrystal growth: (i) sectioning along $(2\bar{1}1)$ and removal from the stem; (ii) and (iii) sectioning along $(0\bar{1}1)$, half removed; (iv) $(2\bar{1}1)$ section matched with $(0\bar{1}1)$ section; and (v) local melting to fuse the horizontal gap.

Fig. 5: Preparation of "match-up" seed for symmetrical bicrystals: (i) single crystal with [011] direction tilted from the cylinder axis; (ii) sectioning along (hkl) and horizontal cut at the middle of the split cylinder; (iii) right halves of both cylinders removed; (iv) upper left half cylinder rotated about the cylindrical axis by 180° and matched with the lower left half; and (v) local melting to fuse the horizontal gap.

Fig. 6: Schematic illustration showing preparation of symmetrical
bicrystals with tilt boundaries: (i) single crystal seed
with longitudinal reference mark; (ii) crystal cut perpen-
dicular to the cylindrical axis, the upper crystal rotated
by 180°; (iii) rejoining by local melting; and (iv) bound-
ary elevated to eliminate voids at the interface. The
method is not applicable if the cylindrical axis has a
rotational symmetry. (Cheng and Chou [5].)

Fig. 7: Schematic illustration showing preparation of bicrystals
with twist boundaries: (i) single crystal with longitudinal
reference mark; (ii) transverse cut and rotation about the
cylindrical axis by a preassigned angle; (iii) rejoining by
local melting; and (iv) elevation of boundary to eliminate
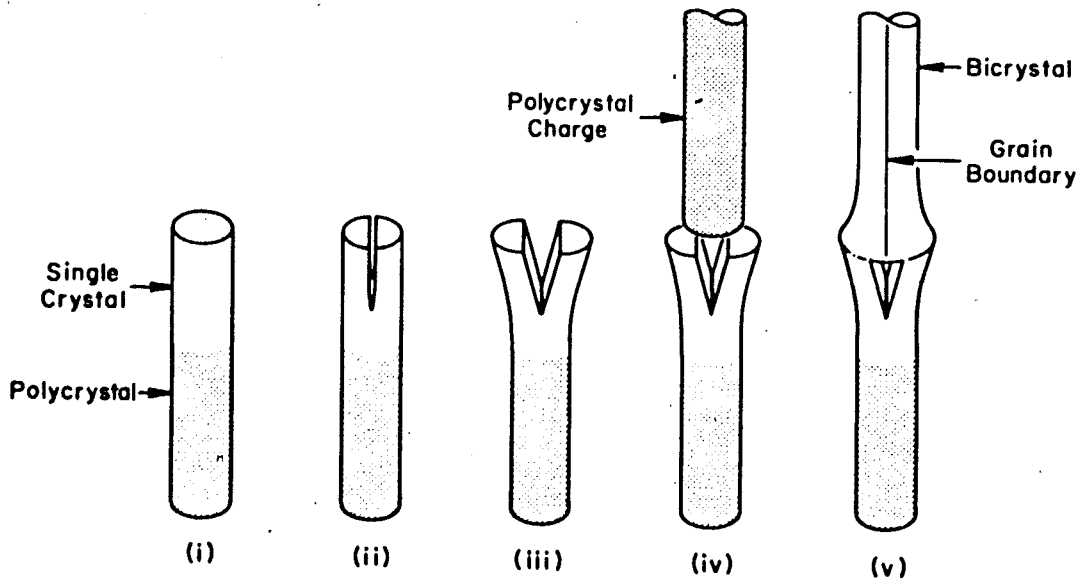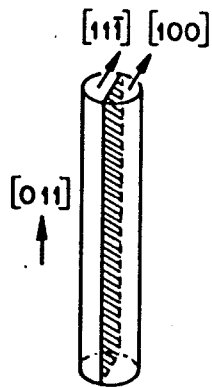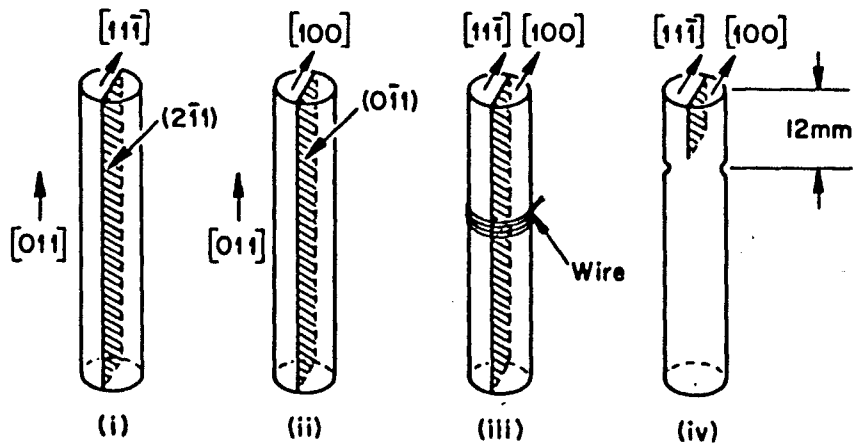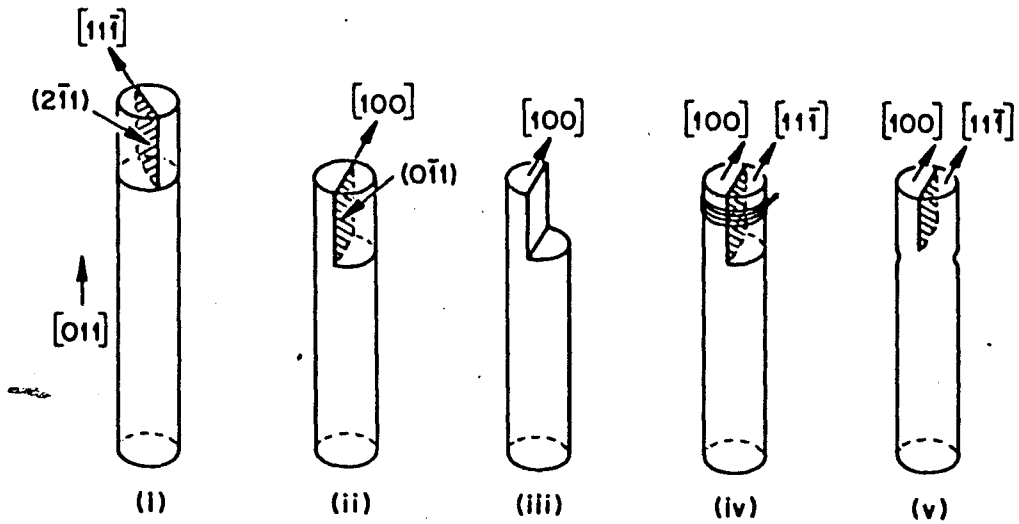voids at the interface. (Cheng and Chou [5].)

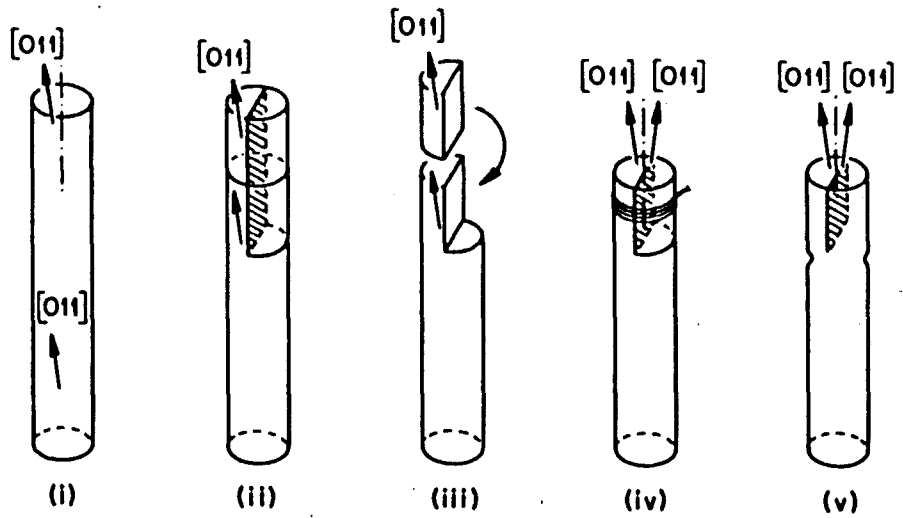**Fig. 1**
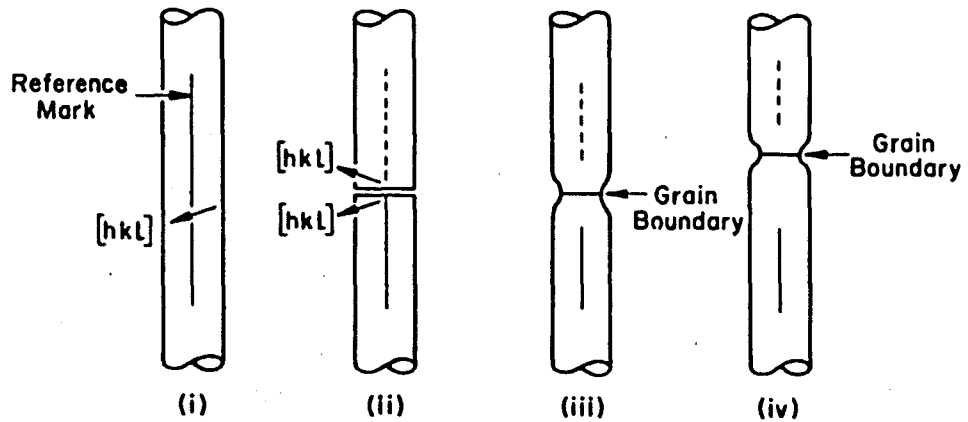

Fig. 2

Fig. 3

Fig. 4
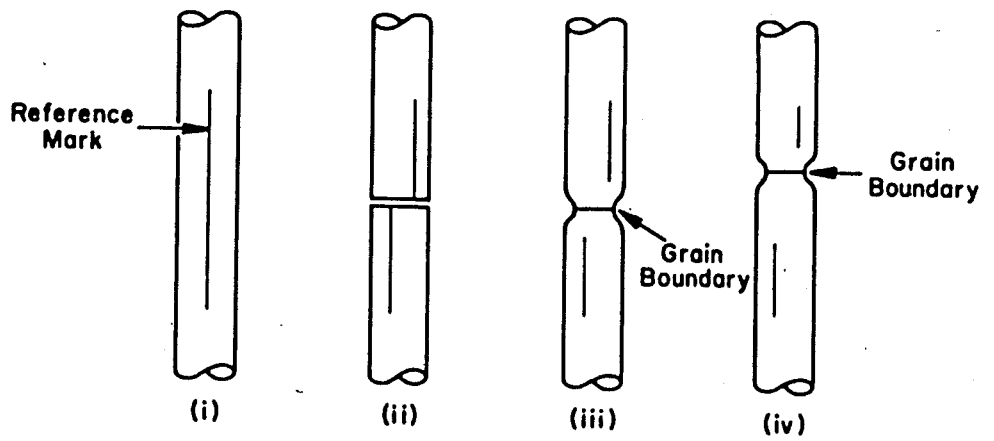
Fig.5

Fig.6

Fig. 7

PART 2

Etch Pits on Single Crystals and Bicrystals of Niobium

1. Introduction

Etch pits were observed on the surface of niobium crystals by several authors during their studies of the motion of dislocations. The etch pits on the {111} planes were reported to be triangular [1-3], while the pits on the {112} planes were reported to be of a pennant shape [4]. More recently, Baranova [5], using a new etching solution, observed lenticular pits on the {013} planes and triangular pits on the {111} planes.

This note reports a detailed study of etch pits on niobium single crystals and bicrystals. The procedure for revealing the etch pits is given in Section 2. In Section 3, it will be shown that the shapes of the etch pits are related to the orientation of the surfaces on which the pits develop. The shape of a pit depends on its surface position in the unit stereographic triangle ([100]-[110]-[111]) and can be explained by the surface energy concept. In addition, it is possible from the characteristic lines of etch pits to determine the misorientation of tilt boundaries in bicrystals. The details are included in Section 3.

2. Experimental Procedure

The specimens used in this study were niobium single crystals and bicrystals with tilt and twist boundaries. These crystals were grown in a vertical floating-zone electron beam melting furnace [6,7] and contain 130 ppm oxygen, 7 ppm nitrogen, 5 ppm hydrogen, 20 ppm carbon, 410 ppm tantalum, and 65 ppm tungsten. Each of the as-grown specimens was mechanically ground through 600-grade emery paper and chemically polished in a solution containing equal volume of HNO_3 and HF for 30 seconds at room temperature.

The critical step in developing etch pits is the exposure to a suitable etching solution. The etchant used in the present investigation is a modification of the etching solution used by Baranova [5]. It contains 60 ml HF (48% conc.), 40 ml H_2O_2 (30% conc.), and 0.55 g NaF. The etching time was 5 minutes at room temperature.

After the etch pits were produced and photographed, the surface was reground for the determination of the surface orientation by the Laue back-reflection x-ray technique. A qualitative correlation was established between the morphology of the etch pits and the orientation of the etching surface.

3. Results and Discussion

A. Observation of Etch Pits on Single Crystals

The etch pits observed on niobium single crystals range from triangular to bricklike in shape, depending on the orientation of the etching surface. Etch pits, developed on the {111} planes, were in the shape of an equilateral triangle (Fig. 1). The shape of pits on planes deviating from the {111} plane changed gradually (Fig. 2). No etch pits were visible on the {110} planes. However, when the etching surface was inclined to the {110}, the pits appeared. Figure 3 shows the brick-like etch pits on a plane, 8° from the {110} plane. No etch pits were visible on the {100} planes, but when the etching surface was inclined to the {100}, lenticular pits were observed (Fig. 4).

Etch pits on other planes along and inside the unit stereographic triangle ([100]-[110]-[111]) are shown in Figure 5. When the plane rotates from a {111} to {110}, the shape of the pits changes from that of an equilateral to an isosceles triangle. As the rotation increases,

the length of the two equal sides of the isosceles triangle becomes increasingly shorter, and, finally, the pits become bricklike. However, when the plane changes from a {111} to a {112}, the shape of the etch pits also becomes isosceles triangular, but with the equal sides extended. Upon reaching the {112} plane, the pits become lenticular, as shown in Figure 4.

From the above observations, it is apparent that the shapes of the etch pits are orientation dependent. For a given plane, a certain type of etch pit appears to occur. It is worth noting that there is no correlation between the direction of the dislocation lines (with respect to the surface) and the shape of the etch pits. The presence of dislocations merely initiates the etch pits as a result of high strain energy and/or their association with impurities and precipitates.

To understand why the shape of the etch pits varies with crystallographic planes, it is useful to introduce the concept of minimum surface energy. It is well-known that the atomically densest plane has the lowest surface energy and the highest resistance to chemical attack. In b.c.c. metals the {110} planes are the most closely packed. Thus one should expect that the {110} planes would be the least attacked and the most stable and would, therefore, form the three sides of a tetrahedral pit which intersect with the {111} base plane, resulting in an equilateral triangular shape on the etching surface.

The above assumption can be verified experimentally. From the geometry of a {110}-sided-{111}-base tetrahedron in a cubic crystal, the ratio of the height of the tetrahedron to its {111}-base plane can be calculated to be $\sqrt{6}/12$, or 0.204 (Appendix A). However, direct measurement of the height by experiment is difficult. Instead, an indirect

-21-

evaluation was made by comparing the shape change from the {111} pit[*] to a pit whose surface is inclined slightly to the {111} plane. The details are described in Appendix B. Indirect measurement gives a value of 0.206, which is in good agreement with the theoretical value of 0.204.

The above assumption is also supported by the change in shape of a {110}-sided-{111}-base tetrahedral pit. When the etching surface tilts from the <111> to the <100> pole, the triangular characteristics of the {110}-sided pit should be lost totally when the tilt angle reaches 19.47° (Appendix C). As shown in Figure 4, the etch pits on the {112} plane are of lenticular shape and there is no trace of triangular pits. The angle between [111] and [112] is 19.5°, slightly greater than 19.47°.

Based on the assumption that the etch pit is a tetrahedron composed of three {110} sides with a {111} base, the observed geometry of etch pits on niobium single crystals can be explained. When the etching surface is a {111} plane, three symmetrical {110} planes can intersect with it (Fig. 6). The shape of the pit is then an equilateral triangle. When the etching surface deviates from a {111} plane, the cross-section through the pyramid defined by the three {110} planes deviates from an equilateral triangle, as shown in Figure 2. When the surface of the specimen is a {110} plane, etch pits form with difficulty because there are no other {110} planes that intersect the {110} surface at an acute angle. This is noted in Reference 3 and is supported in the present study. As the surface of the specimen deviates from a {110} plane, other {110} planes come into coincidence, making acute angles with the

_____

[*] By a {111} etch pit, we mean that the etching surface is a {111} plane.

etching surface, and etch pits are developed. However, to show the intersecting {110} planes in a pit by metallography, the angle of deviation should not be too small. Figure 3 shows the pits on a plane about 8° from a {110} plane. The intersecting {110} planes in the pits are clearly visible.

From Figure 6, it can be expected that when the etching surface tilts from a {111} plane to a {110} plane, the triangle becomes isosceles, and that the length of the two equal sides becomes increasingly shorter on approaching a {110} plane. Likewise, as the etching surface tilts from a {111} to a {100}, the equal sides of the isosceles triangle become increasingly longer. These expectations are in agreement with experimental observations.

It should be noted that the relative surface energies of various crystallographic planes can be altered by the presence of impurities and alloying elements and by the chemical composition of the etching reagent. Thus, the same type of etch pits observed in pure niobium may not occur in its alloys or in other metals. For example, etch pits in tungsten were found to develop only on those surfaces which are inclined up to 38° to a {100} plane [8]. In Cu-Al alloys [9], f.c.c. in crystal structure, the shape of etch pits on the {111} planes changes from that of an equilateral triangle for pure copper to that of a rounded ellipse for a Cu + 2.5% Al alloy.

B. Observation of Etch Pits on Bicrystals

Bicrystals of both tilt and twist boundaries were examined. Etch pits were produced on surfaces perpendicular to the grain boundary planes. For tilt boundary bicrystals, the etching surfaces are also

-23-

perpendicular to the tilt axes. Figure 7 shows the etch pits on the ($1\bar{1}1$) plane of a [011]/[$1\bar{1}1$] bicrystal with a symmetric tilt boundary.* The boundary has a misorientation of 22°, as measured by the Laue back-reflection x-ray technique. Etch pits were also grown on the ($1\bar{1}1$) plane of a second [011]/[$1\bar{1}1$] bicrystal of 25° misorientation, as shown in Figure 8. Figure 9 illustrates etch pits on the ($21\bar{1}$) plane of a [011]/[$21\bar{1}$] bicrystal with a misorientation of 19°. The ($21\bar{1}$) pits are not lenticular, as expected, because the specimen was over-etched deliberately to enlarge the pits for accurate measurement of their angles. In this case, the misorientation can be determined simply by the change in direction of the elongated pits as they cross the grain boundary. Figure 10 shows the etch pits on a bicrystal of twist boundary with a misorientation of 70°.

Based on the geometry of the pits on niobium single crystals discussed above, it is possible to use the etch pit technique to determine the misorientation of tilt boundary bicrystals. At this point, it is useful to introduce the term, "<112> characteristic lines." For a {110}-sided-{111}-base tetrahedron, the intersecting line of two {110} planes is the <111> direction and its projection on the {111} plane is along <112>. This projection line will be referred to as the "<112> characteristic line." For convenience, one may also use the term "characteristic line" for the projection

_____

*The designation refers to bicrystals grown from the Y-shaped seeds. The first vector indicates the symmetrical pair of vectors that span the misorientation angle of the bicrystal. The second vector indicates the tilt axis.

lines of <111> on any other etching plane. In such cases the pre-term <112> is omitted.

Referring to Figure 11, let the misorientation of the tilt boundary be designated by $\theta_1 + \theta_2$, where θ_1 and θ_2 are the angles between the normal of the boundary plane and the <112> characteristic line of the etch pit in crystal 1 and crystal 2, respectively. By the etch pit technique, the values of θ_1 and θ_2 can be measured. In Figure 7, θ_1 and θ_2 and both 11°, and the grain boundary is symmetrical. In Figure 8, θ_1 and θ_2 are 15° and 10°, respectively. The boundary is, therefore, an asymmetrical tilt boundary of misorientation 25°. These results are consistent with those measured by the Laue back-reflection technique. In Figure 7, the etch pits on the left crystal deviate slightly from equilateral triangles in shape due to an inadequately prepared etching surface. However, it still may be concluded that the etch pits on both sides of the boundary have the same shape, as the corresponding pair of <112> characteristic lines of pits in both crystals are symmetrical about the normal of the boundary plane. This method, however, is not valid for bicrystals with [100] and [110] tilt axes, because of the difficulty of producing etch pits on {100} and {110} planes.

The etch pit technique may be used as a guide to distinguish the type of the boundary in a bicrystal. This can be illustrated by the following example: A bicrystal was grown accidentally on a single crystal of niobium. The boundary of the bicrystal was parallel to the growth direction, [011]. Etch pits were produced on the surface, cut parallel to the growth direction and perpendicular to the bound-

-25-

ary plane (Fig. 12). From the photograph in Figure 12, it can be seen that two of the characteristic lines, one from each crystal, are parallel to each other but perpendicular to the boundary plane. This indicates that the [011] directions of crystal 1 and crystal 2 are both parallel to the boundary plane and the growth direction. Since [011] is the common direction, it must be a tilt boundary. From these features, one would expect that this bicrystal with a tilt boundary would be grown accidentally as the result of a relative rotation of the left and right half crystals around the [011] growth direction. This expectation was indeed confirmed by the x-ray diffraction patterns included with the etch pit pattern in Figure 12. However, since the tilt axis is not perpendicular to the etching surface, it is no longer possible to measure the boundary misorientation by the directional change of the characteristic lines between crystal 1 and crystal 2.

4. Conclusions

1. Three different types of etch pits were observed in single crystals of pure niobium based on the position of the etching surface in the unit stereographic triangle. The shape of the pits is clearly orientation dependent.

2. It was assumed that the {110} planes, which have the lowest surface energy in b.c.c. metals, are the most stable during etching of niobium. The concept of minimum surface energy has been used successfully to explain the crystallographic geometry of etch pits in niobium single crystals and bicrystals.

-26-

3. The etch pit technique may be used to determine the misorientation of a tilt-boundary bicrystal by the directional change in the etch pit characteristic lines. This allows one also to determine qualitatively the type of boundary in a bicrystal (whether twist or tilt, symmetric or asymmetric).

References

1. P. R. Evans, J. Less-Common Metals, 6, 235 (1964).

2. W. F. Sheely, J. Less-Common Metals, 2, 399 (1960).

3. E. Zedler, J. of Applied Physics, 38, 2046 (1967).

4. H. D. Guberman, Oak Ridge National Laboratory Report No. 3879, 1966, p. 49.

5. G. K. Baranova, Scripta Met., 11, 827 (1977).

6. C. S. Pande, L. S. Lin, S. R. Butler and Y. T. Chou, J. of Crystal Growth, 19, 209 (1973).

7. B. C. Cai, A. DasGupta and Y. T. Chou, submitted to J. Less-Common Metals, (1982).

8. U. E. Wolff, Acta Met., 6, 559 (1958).

9. J. Watanabe and S. Sugawara, J. Japanese Institute of Metals (in Japanese), 41, 612 (1977).

Appendix

A. Computation of the height-to-base ratio of a {111} tetrahedral pit.

For a tetrahedron composed of three {110} planes as sides and one {111} plane as base in a unit cube of cubic symmetry, the height, DE (Fig. 13a), is given by

$$DE = AD \sin\theta = \frac{\sqrt{6}}{4} AB \sin\theta, \qquad (A\ 1)$$

where AD is half of the cube diagonal, AB is the diagonal of the cubic face, and θ is the angle between the [111] and [112] axes. Hence the ratio,

$$\frac{DE}{AB} = \frac{\sqrt{6}}{4} \sin\theta = \frac{\sqrt{6}}{12} = 0.204 \qquad (A\ 2)$$

B. Experimental evaluation of the height-to-base ratio for a {111} tetrahedral pit.

A {111} tetrahedral pit is composed of three identical sides and an equilateral triangular base. To prove that the three sides are {110} planes, it is necessary to show that the ratio of the height to the base of the tetrahedron is $\frac{\sqrt{6}}{12}$ ($= 0.204$).

Because of the small size of the tetrahedral pit, direct measurement of the ratio is difficult. However, indirect evaluation can be made by measuring the size of the isosceles triangular pit on an etching surface tilted from the {111} plane by the tilt angle φ (Fig. 13a).

Consider Section CDF of the {111} pit and Section C'D'F' of the pit inclined by an angle φ from the {111} plane (Fig. 13b). Since the base ABC of the tetrahedron is an equilateral triangle and its three sides are symmetrical about the axis of the tetrahedron, the angles α and β are determined only by the height DE and base AB. For simplicity of analysis, let us consider an equivalent case in which the CEF and C'E'F' are made

-28-

coincident (Fig. 13c). The two vertices D and D' are then separated and D'E = DE. From Figure 13d, it can be seen that

$$D'E' = D'E \cos \varphi = \frac{\sqrt{3}}{3} AB \cot \alpha \cos \varphi \qquad (A\ 3)$$

$$E'F' = D'E' \cot(\beta + \varphi) \qquad (A\ 4)$$

and

$$EF' = EE' + E'F' = \frac{\sqrt{3}}{3} AB \cot\alpha [\cot(\beta + \varphi)\cos \varphi + \sin \varphi] \qquad (A\ 5)$$

When φ is small, it is permissible to assume that $\triangle ABE$ and $\triangle A'B'E'$ are similar.

Hence

$$A'B' = 2AB \cot \alpha [\cot(\beta + \varphi)\cos \varphi + \sin \varphi] \qquad (A\ 6)$$

and

$$\frac{A'B'}{E'C'} = 2\sqrt{3} \frac{\tan \alpha \sec^2 \varphi (1 - \tan \alpha \tan \varphi)}{(\tan \alpha + \tan \varphi)(2 + \tan \alpha \tan \varphi)} \qquad (A\ 7)$$

In equation (A 7), the value of the ratio A'B'/E'C' can be measured on microphotographs of the etching surface, and the angle φ by the back-reflection Laue patterns.

For the case where $\varphi = 9°$ and A'B'/E'C' = 0.77, the value of tan α is found to be 2.8 and, consequently,

$$\frac{DE}{AB} = \frac{\sqrt{3}}{3} \cot \alpha = 0.206 \qquad (A\ 8)$$

The above result is in good agreement with the theoretical value of 0.204 for a {110}-sided-{111}-base tetrahedral pit.

C. Condition for disappearance of triangular pits

It is seen from Figure 13b that the two equal sides of the isosceles triangular pit increase in length as the angle φ increases. When φ reaches its limiting value of 19.47° (=90° - α), the point C' is extended infinitely and the triangular pit no longer exists.

Figure Captions

Fig. 1: Etch pits on a {111} plane. 800X.

Fig. 2: Etch pits on a plane deviated from {111} plane. 400X.

Fig. 3: Etch pits on a plane inclined by 8° from {110} plane. 500X.

Fig. 4: Etch pits on a {112} plane. 200X.

Fig. 5: Orientation dependence of etch-pit shapes.

Fig. 6: Schematic representation of a three dimensional etch pit. The tetrahedral pit is composed of three {110} planes with a {111} plane as the etching surface.

Fig. 7: Etch pits on plane perpendicular to [1̄1̄1] tilt axis of a symmetric bicrystal. The misorientation angle θ = 22°.

Fig. 8: Etch pits on a plane perpendicular to [1̄1̄1] tilt axis of an asymmetric bicrystal. θ = 25°.

Fig. 9: Etch pits on a plane perpendicular to [21̄1̄] tilt axis of a symmetrical bicrystal. θ = 19°. 500X.

Fig. 10: Etch pits on both sides of a twist grain boundary. 400X.

Fig. 11: Schematic diagram showing the orientation of the etch pits on (1̄11) plane of a bicrystal with symmetric tilt boundary. Tilt axis along [1̄1̄1].

Fig. 12: Etch pits on a bicrystal of natural growth. 400X. The Laue back-reflection x-ray patterns for the two crystals are included on the two sides for comparison.

Fig. 13: Schematic diagram showing the geometry of a {110}-sided-{111}-base tetrahedron after tilt by an angle φ about <110> axis.
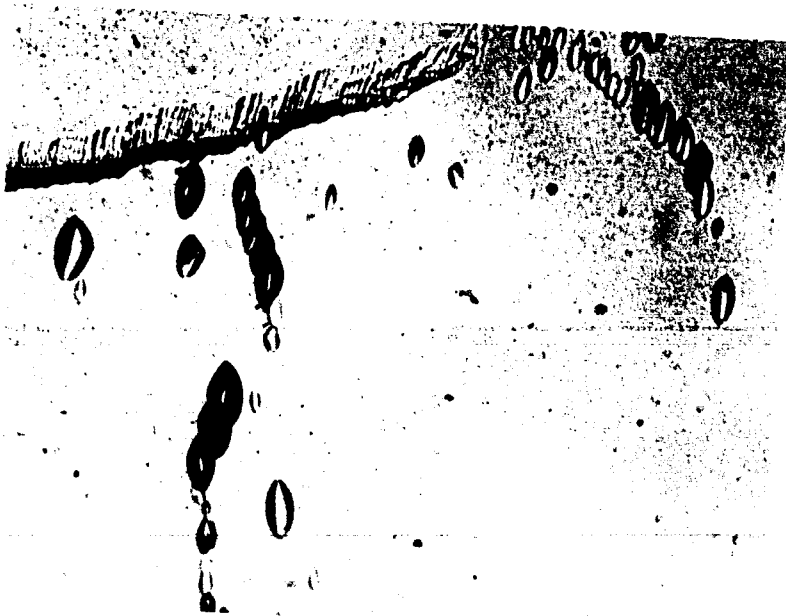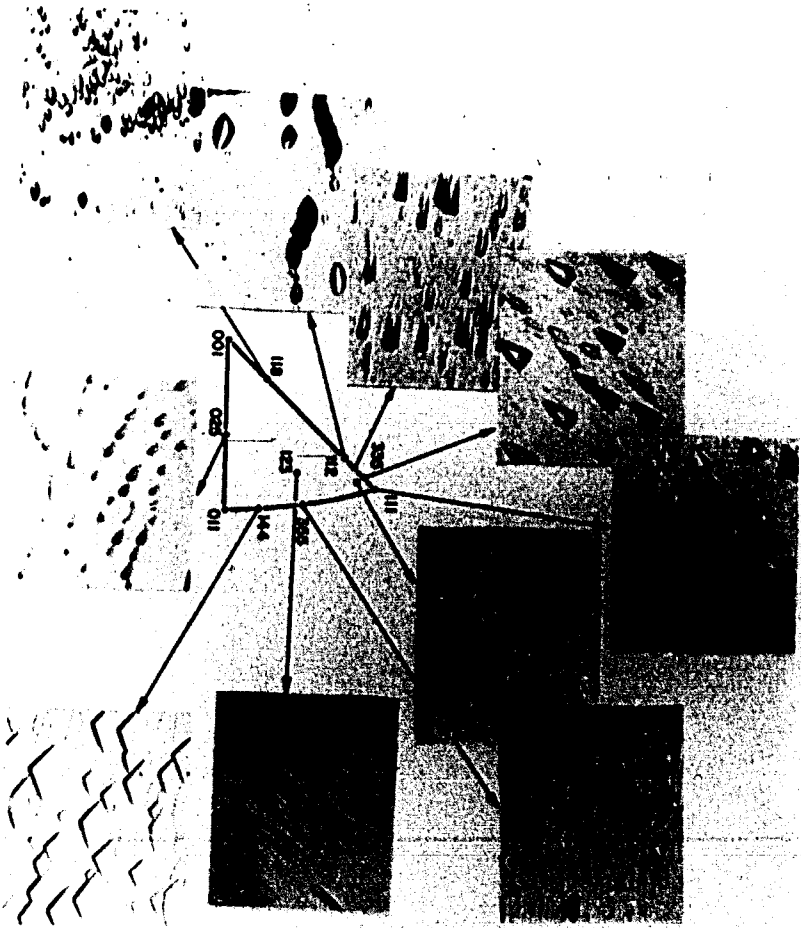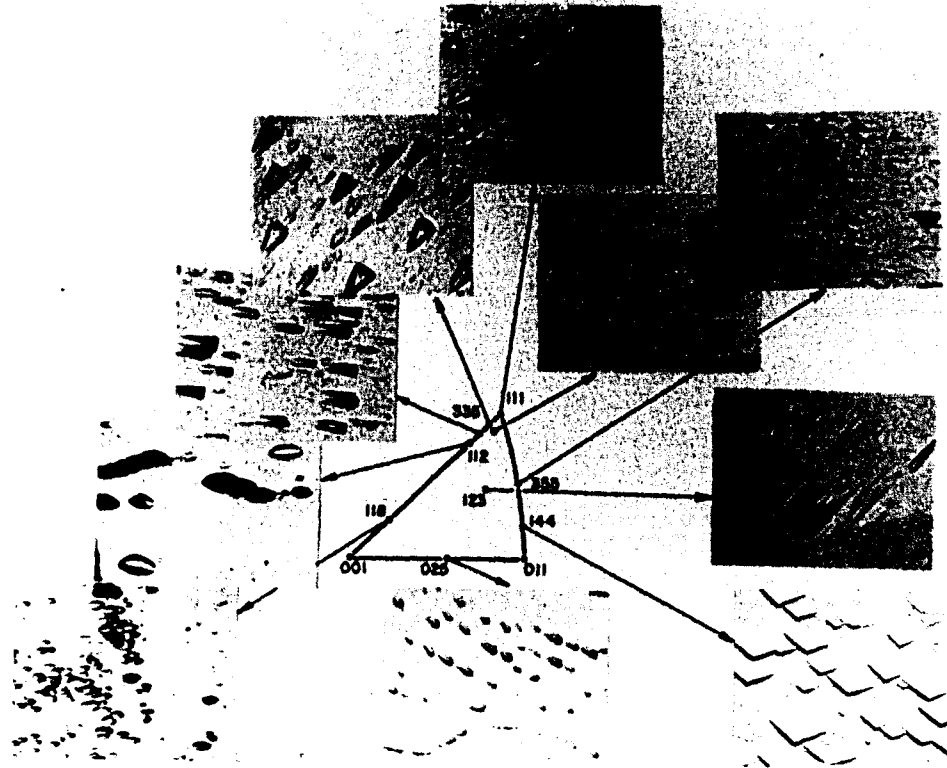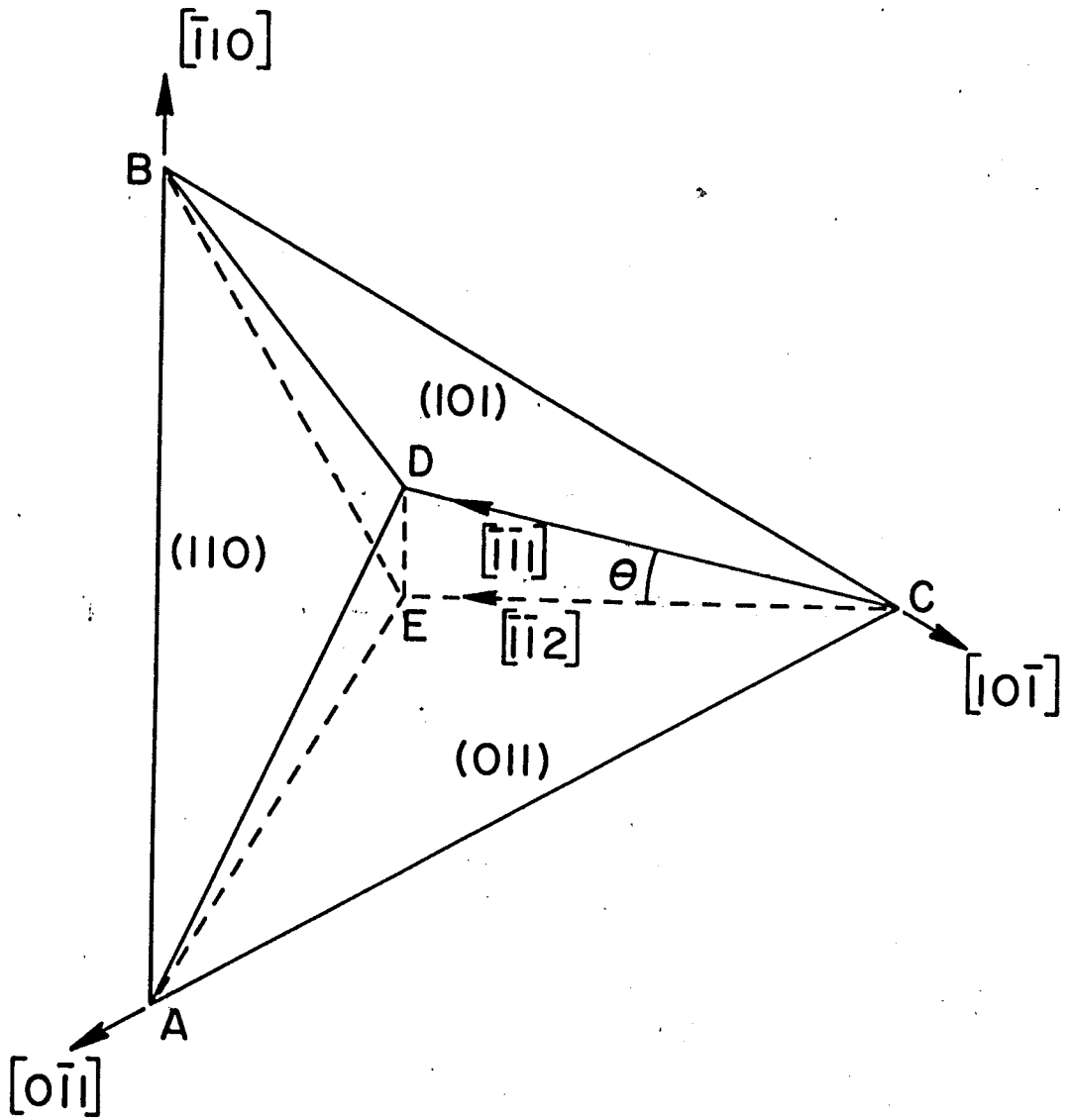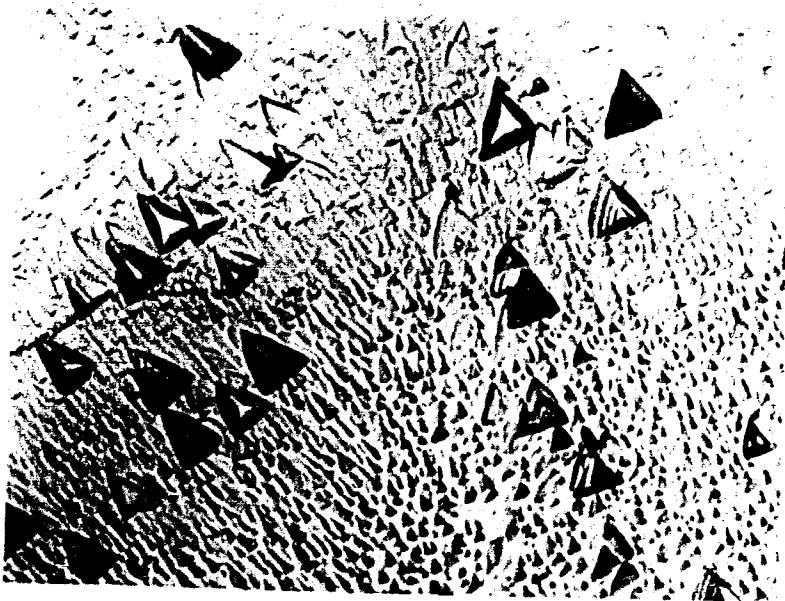
Fig. 1

Fig. 2

-31-
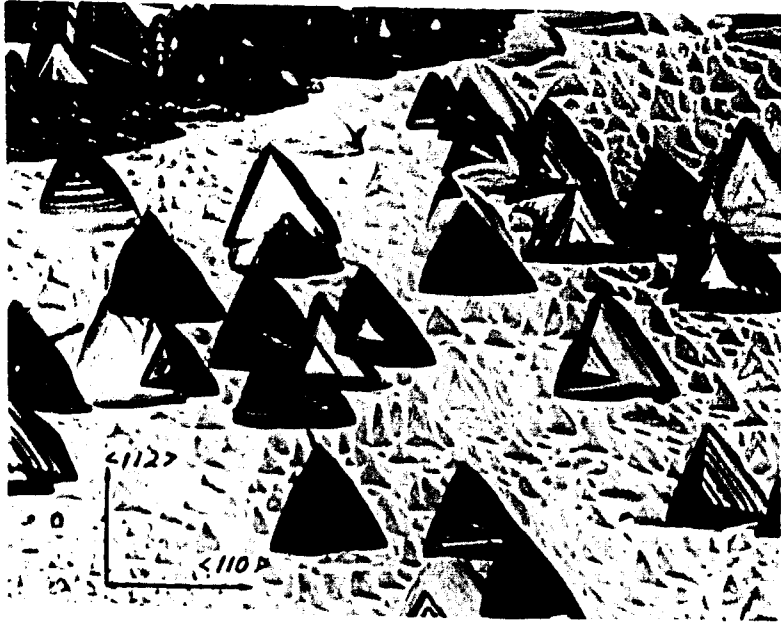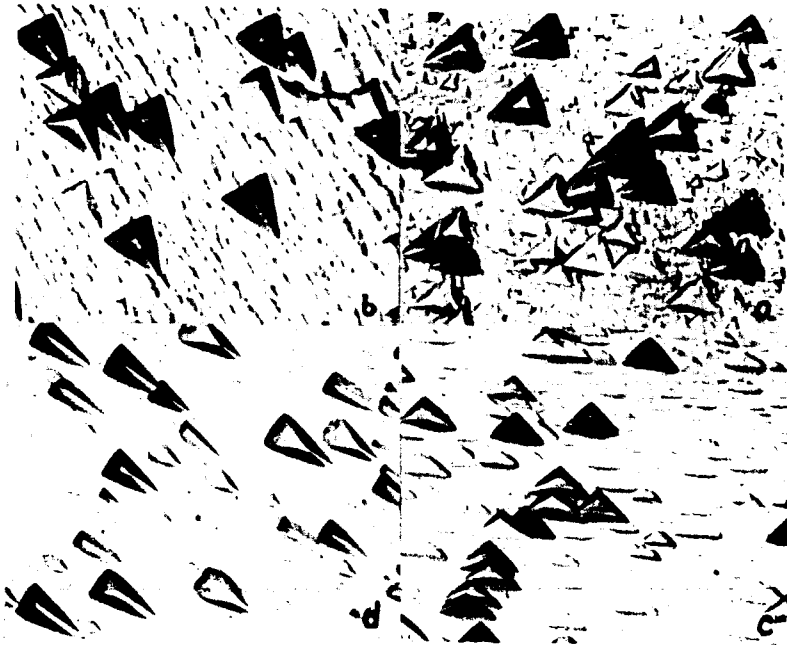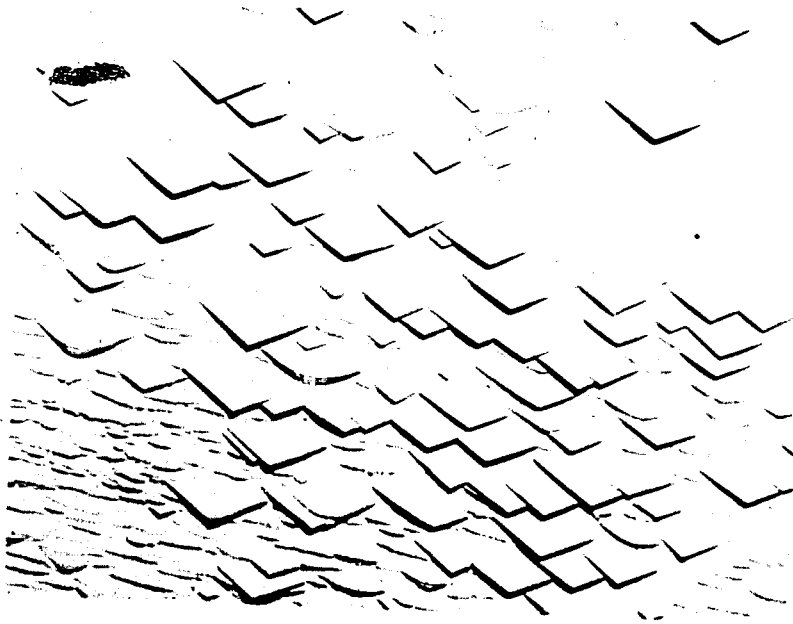
Fig. 3

Fig. 4

Fig. 5

Fig. 5

Fig. 6

Fig. 7

Fig. 8

Fig. 9

Fig. 10

GRAIN
BOUNDARY

$[21\bar{1}]$

θ_1

$[21\bar{1}]$

θ_2

BICRYSTAL

θ_1

$[21\bar{1}]$

$[21\bar{1}]$

θ_2
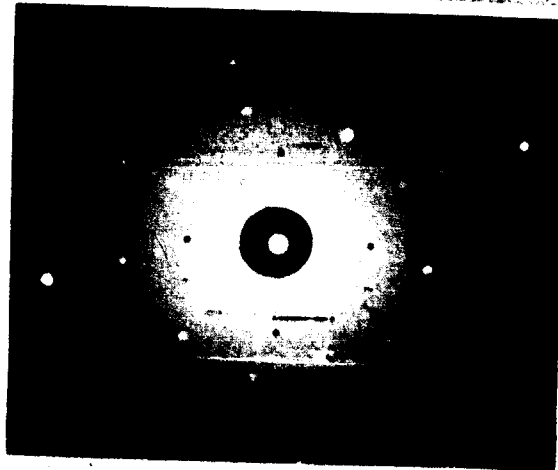
$[011]$
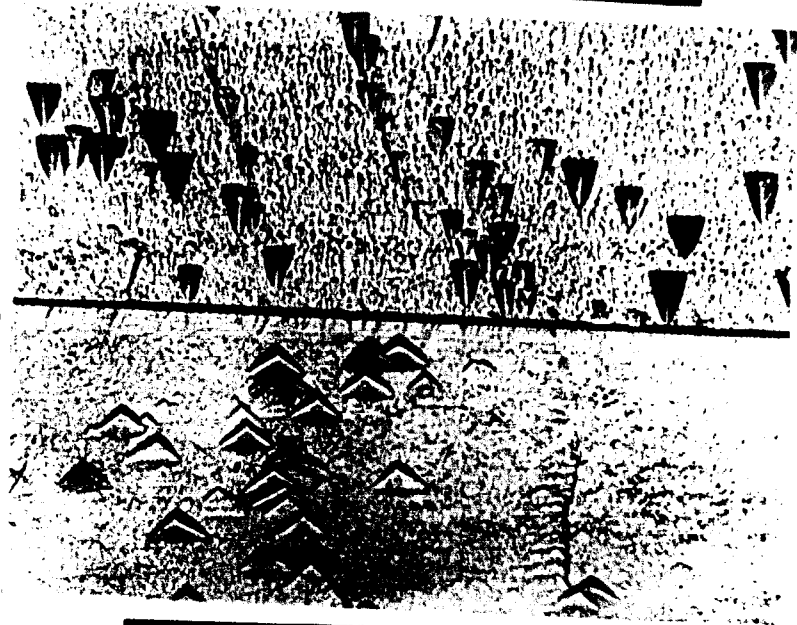
$[21\bar{1}]$

SINGLE
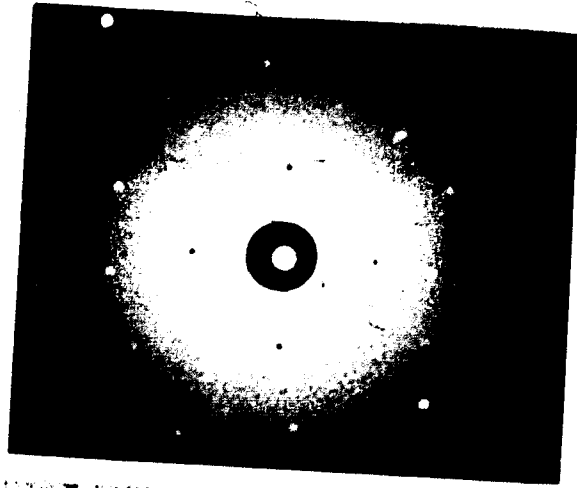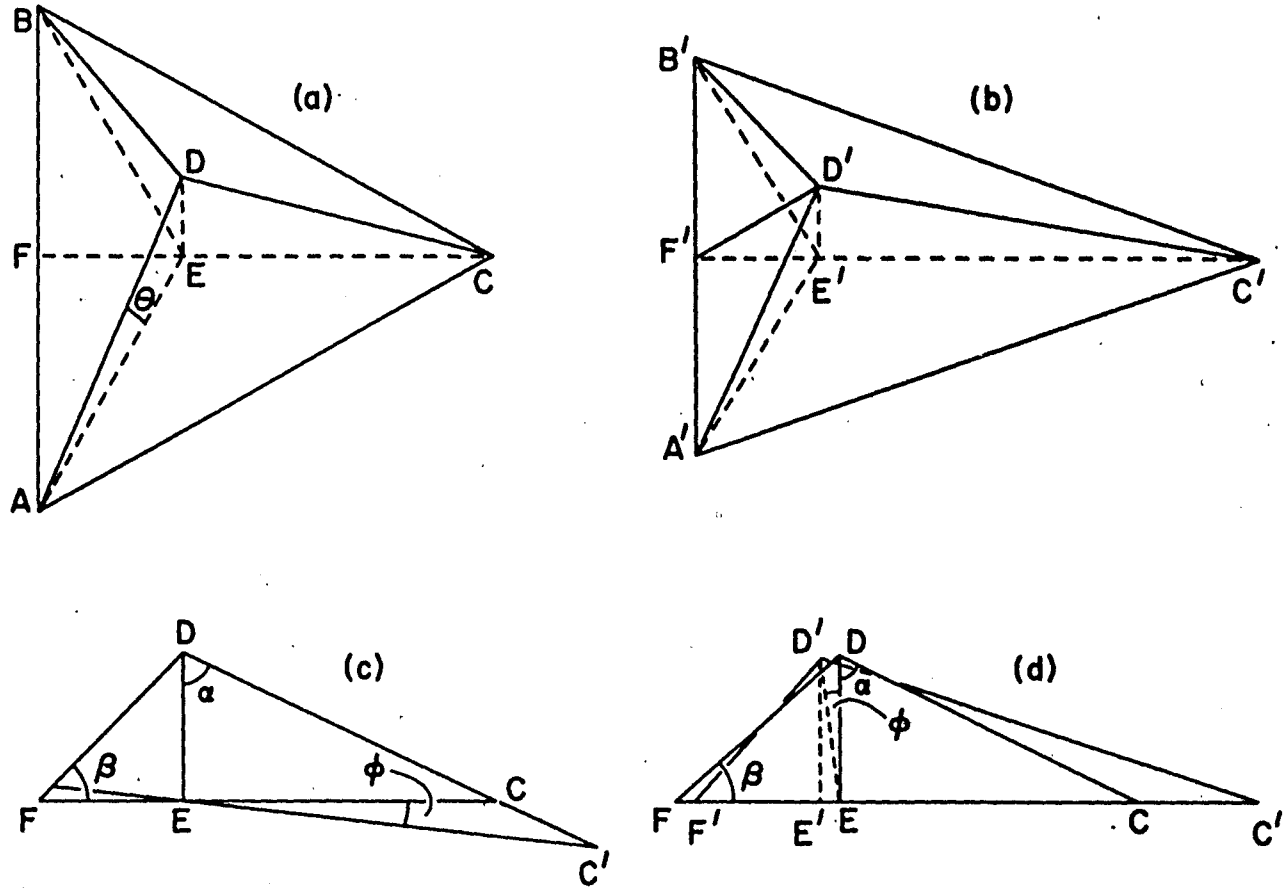CRYSTAL

-37-
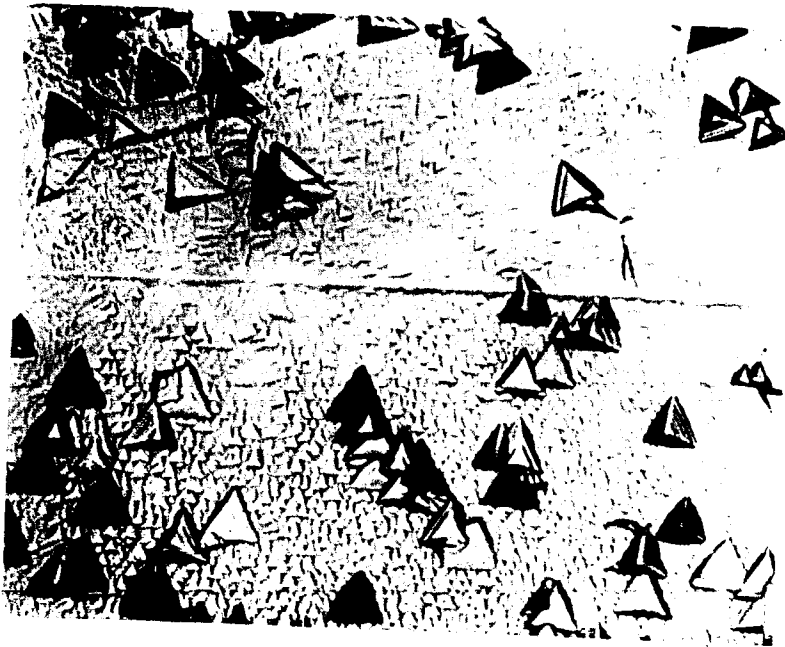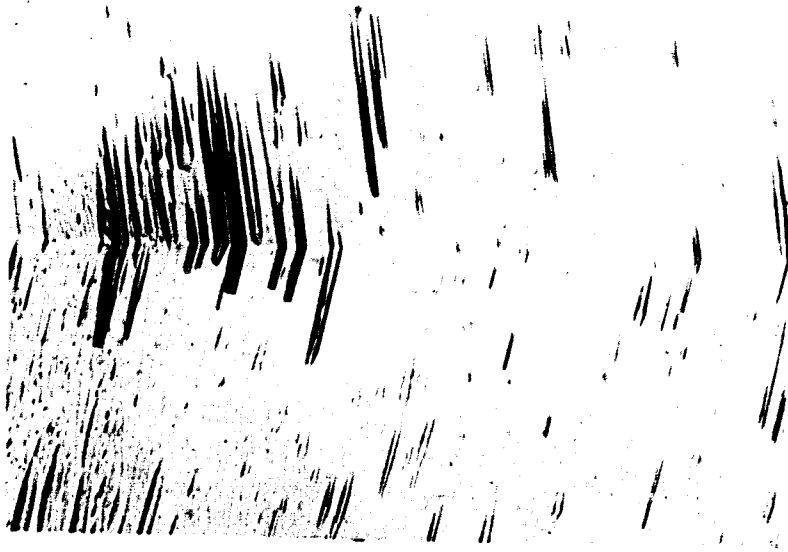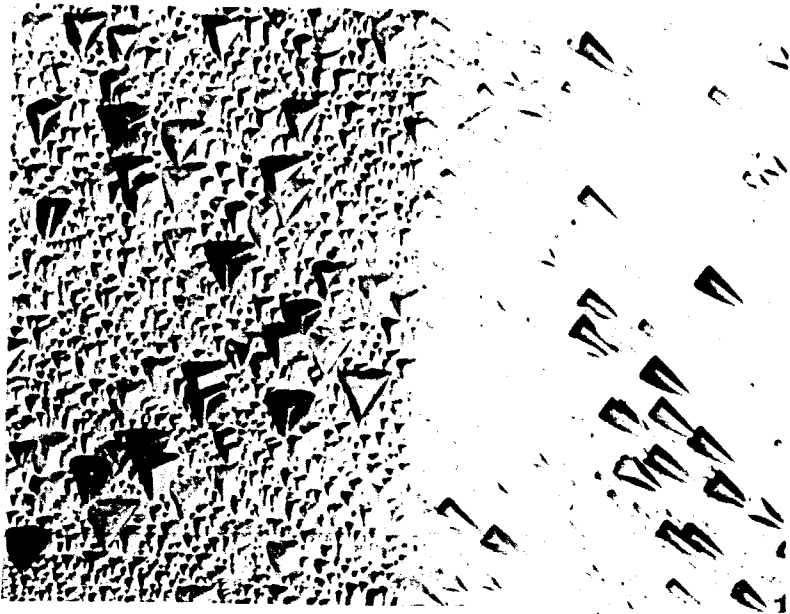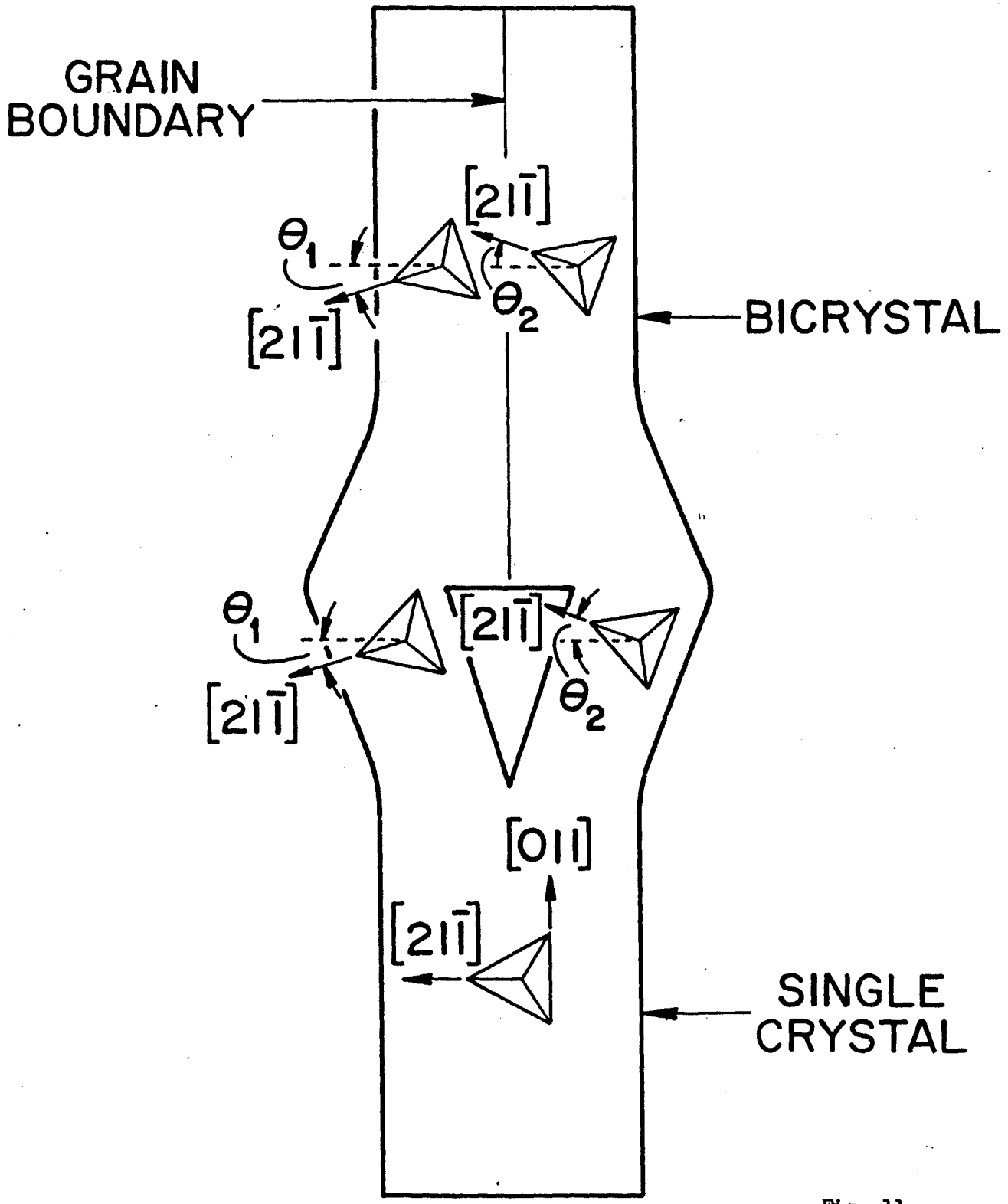
Fig. 11

Fig. 12

Fig. 13

PART 3

Correlation Between Grain Boundary Hardening

and

Grain Boundary Energy in Niobium Bicrystals

1. Introduction

Microhardness measurements have been used in recent years in the study of grain boundary properties (Westbrook 1964). The hardness readings at a grain boundary are generally higher than those in the grain (Westbrook and Aust 1963, Aust, Hanneman, Niessen and Westbrook 1968, Raghuram, Reed and Armstrong 1969, Braunovio and Haworth 1972, Watanabe, Kitamura and Karashima 1980). Such excess hardening is believed to be caused by boundary segregation of solute atoms; this segregation plays an important role in grain boundary embrittlement (Stein, Joshi and LaForce 1969, Banerji, McMahon and Feng 1978) and grain boundary corrosion (Arora and Metzger 1966, Qian and Chou 1982).

The structure dependence of boundary hardening in bicrystals of zone-refined lead alloys containing ppm concentrations of Sn, In, Ag, and Au has been investigated by Westbrook and Aust (1963). They noted that the boundary hardening was maximum for high angle boundaries and was small or undetectable for low angle boundaries. More recently, Watanabe, Kitamura and Karashima (1980) completed a detailed study on misorientation dependence of boundary hardening in coarse grained Fe + 1.08 at.% Sn alloy. This study determined that boundary hardening is misorientation dependent and is enhanced by the boundary segregation of tin. Furthermore, boundary hardening was found to be very small near the coincidence site lattice boundaries with $\Sigma = 3$ and 7 (Pande and Chou 1975, Pumphrey 1976).

The objective of this investigation was to obtain new data on boundary hardening in b.c.c. metals. Niobium bicrystals have been chosen as the model material. An important aspect of the present study is that the

boundary structure is precontrolled, thus making it possible to provide a direct correlation between grain boundary hardening and grain boundary energy.

2. Experimental Procedure

Niobium bicrystals with symmetric tilt boundaries were grown in a vertical floating zone electron beam melting furnace using the Y-shaped seed method developed by Pande, Lin, Butler and Chou (1973). Four sets of bicrystals were prepared, designated by [011]/[100], [011]/[01$\bar{1}$], [011]/[11$\bar{1}$], and [001]/[100] bicrystals, where the first vector represents the misorientation vector and the second represents the tilt axis.[*] The major impurity contents in a typical bicrystal are: 7 ppm nitrogen, 130 ppm oxygen, 5 ppm hydrogen, 20 ppm carbon, 410 ppm tantalum, and 65 ppm tungsten.

Specimens for microhardness measurement were cut from the bicrystal rods and mounted in polyethylene as the supporting material. The surface of each specimen was prepared by grinding on emery paper through 3/0 grit and polishing in a chemical solution (70% HNO_3 + 30% HF) to remove both the distorted layer and the scratches.

Microhardness was measured with a Reichart microhardness tester which utilized a diamond pyramid indenter under a constant load of 5 grams and a loading time of 5 seconds. The small load was chosen to distinguish the boundary effect from the grain. Measurements with a load of less than

---

[*] The misorientation vector designates the symmetrical pair of vectors that span the misorientation angle of the bicrystal. The misorientation vector [uvw], misorientation angle (θ), and the tilt axis [hkℓ] form a set of base parameters which can be used to specify a symmetrical bicrystal as a [uvw](θ)/[hkℓ] bicrystal. A general set of symmetric tilt boundary bicrystals in which only θ is varying may be termed simply a [uvw]/[hkℓ] set.

5 grams were unreliable due to the vibration of the tester and surface irregularities. All microhardness measurements were made on surfaces perpendicular to the boundary planes (parallel to the tilt axes) and each data point represents an average of three readings on a given specimen.

3. Results and Discussion

When microhardness was measured as a function of the distance from the boundary, a hardening peak appeared at the boundary plane with a width extended to several microns. A typical microhardness-distance profile is shown in Figure 1.

The misorientation dependence of grain boundary hardening observed in niobium bicrystals is summarized in Figures 2 to 5. The boundary hardening ΔH is defined as the difference between the hardness of the boundary H_b and the hardness of the grain H_g. Figure 6 shows the ΔH versus θ plot for low angle boundary bicrystals with the same tilt axis but different misorientation vectors. The θ-dependence of boundary hardening for bicrystals of the same misorientation vector but with different tilt axes is shown in Figure 7.

The results summarized in Figures 2 to 5 show that for low angle boundaries ΔH increases with increasing of θ. A plot of $\Delta H/\theta$ versus $\ln \theta$ yields the linear relationship shown in the upper left corner of each figure. Such behavior is similar to the relationship between the grain boundary energy and θ proposed by Read and Shockley (1950). However, upon approaching a coincidence site lattice boundary, ΔH decreases sharply, reaches a minimum, and rises again, yielding a boundary hardening cusp (minimum).

Based on the model of the coincidence site lattice (CSL), the first and second CSL boundaries for bicrystals with a $<001>$ tilt axis would

appear at $\theta = 22.6^O$ ($\Sigma = 13$) and $\theta = 28.1^O$ ($\Sigma = 17$), respectively. Figures

2 and 3 show that the observed boundary hardening cusps are located at 23°

and 28.5^O for both [011]/[100] and [001]/[100] bicrystals. For bicrystals

of a <011> tilt axis, the first CSL boundary is at 26.5^O ($\Sigma = 19$), whereas

the observed hardening cusp for [011]/[01$\bar{1}$] bicrystals is at 28.5^O (Fig. 4).

For bicrystals with a <111> tilt axis, the first CSL boundary is located

at $\theta = 27.8^O$ ($\Sigma = 13$). The observed boundary hardening cusp for [011]/[11$\bar{1}$]

bicrystals is at $\theta = 28^O$ (Fig. 5).

It is known that at CSL boundaries, the boundary energy and boundary

segregation are lowered because of good atomic matching (Pumphrey 1976).

The present data show that at the CSL boundaries the boundary hardening is

also lowered. Thus, it would seem that boundary energy, boundary segregation,

and boundary hardening are closely related.

The results summarized in Figure 6 show that bicrystals with the same

tilt axis ([100]) but different misorientation vectors ([001] and [011])

exhibit similar boundary hardening effects. It is noted, however, that

even though the ΔH's are nearly equal at a given θ in these two sets of

bicrystals, the corresponding H_b's (or H_g's) are not equal. The reason for

this effect is not obvious. It would be of interest to investigate if similar

results would be observed in studies of bicrystals with other tilt axis such

as <110> or <111>.

Figure 7 shows that the boundary hardening varies for different tilt

axes with the same misorientation vector. Bicrystals with a [11$\bar{1}$] tilt

axis demonstrate the highest effect and those with a [01$\bar{1}$] tilt axis the

least effect. These results clearly indicate that boundary hardening is

structure sensitive. The hardening sequence descending from <111>,

<100> to <110> may result from the difference in atomic densities of

the boundary planes and consequently difference in the boundary segregations. Unfortunately, the current theories of low-angle boundaries are inadequate to substantiate this view. It is also not possible, because of the high ductility of niobium, to fracture the bicrystals in the Auger electron spectrometer to verify the degree of boundary segregation.

The response of boundary hardening to misorientation as observed above is similar to the response of boundary corrosion in niobium bicrystals reported by Qian and Chou (1982).

4. Conclusions

The grain boundary hardening in oriented niobium bicrystals with symmetric tilt boundaries was determined by use of microhardness measurements. The results can be summarized as follows:

1. The boundary hardening is structure sensitive.

2. For bicrystals with low angle boundaries, the boundary hardening (ΔH) increases with increasing misorientation (θ). A plot of $\Delta H/\theta$ versus $\ln \theta$ results in a linear relationship of the Read-Shockley type.

3. For bicrystals with high angle boundaries, boundary hardening cusps (minima) appear near the coincidence site lattice boundaries.

4. There exists a direct correlation between grain boundary hardening and grain boundary energy.

References

Arora, O. P. and Metzger, M., 1966, Trans. Met. Soc. AIME, 236, 205.

Aust, K. T., Hanneman, R. E., Niessen, P. and Westbrook, J. H., 1968,
Acta Met., 16, 291.

Banerji, S. K., McMahon, C. J. and Feng, H. C., 1978, Met. Trans., 9A, 237.

Braunovic, M. and Haworth, C. W., 1972, J. of Mat. Sci., 7, 763.

Pande, C. S. and Chou, Y. T., 1975, in "Treatise in Materials Science and
Technology," ed. by H. Herman, Academic Press, New York, 8, 43.

Pande, C. S., Lin, L. S., Butler, S. R., and Chou, Y. T., 1973, J. Crystal
Growth, 19, 209.

Pumphrey, P. H., 1976, in "Grain Boundary Structure and Properties," ed.
by G. A. Chadwick and D. A. Smith, Academic Press, New York, Chapter 5
p. 139.

Qian, X. R. and Chou, Y. T., 1982, Phil. Mag. to appear.

Raghuram, A. C., Reed, R. E. and Armstrong, R. W., 1969, J. Appl. Phys.,
40, 4666.

Read, W. T. and Shockley, W., 1950, Phys. Rev., 78, 275.

Stein, D. F., Joshi, A. and LaForce, R. P., 1969, Trans. ASM, 62, 776.

Watanabe, T., Kitamura, S. and Karashima, S., 1980, Acta. Met., 28, 455.

Westbrook, J. H., 1964, Met. Reviews, 9, 415.

Westbrook, J. H. and Aust, K. T., 1963, Acta.Met., 11, 1151.

Figure Captions

Fig. 1. Hardness-distance profile of a $[011]/[11\bar{1}]$ niobium bicrystal with symmetric tilt boundary.

Fig. 2. Variation of ΔH with θ for $[001]/[100]$ bicrystals.

Fig. 3. Variation of ΔH with θ for $[011]/[100]$ bicrystals.

Fig. 4. Variation of ΔH with θ for $[011]/[01\bar{1}]$ bicrystals.

Fig. 5. Variation of ΔH with θ for $[011]/[11\bar{1}]$ bicrystals.

Fig. 6. ΔH versus θ for different mixorientation vectors. Tilt axis along $[100]$.

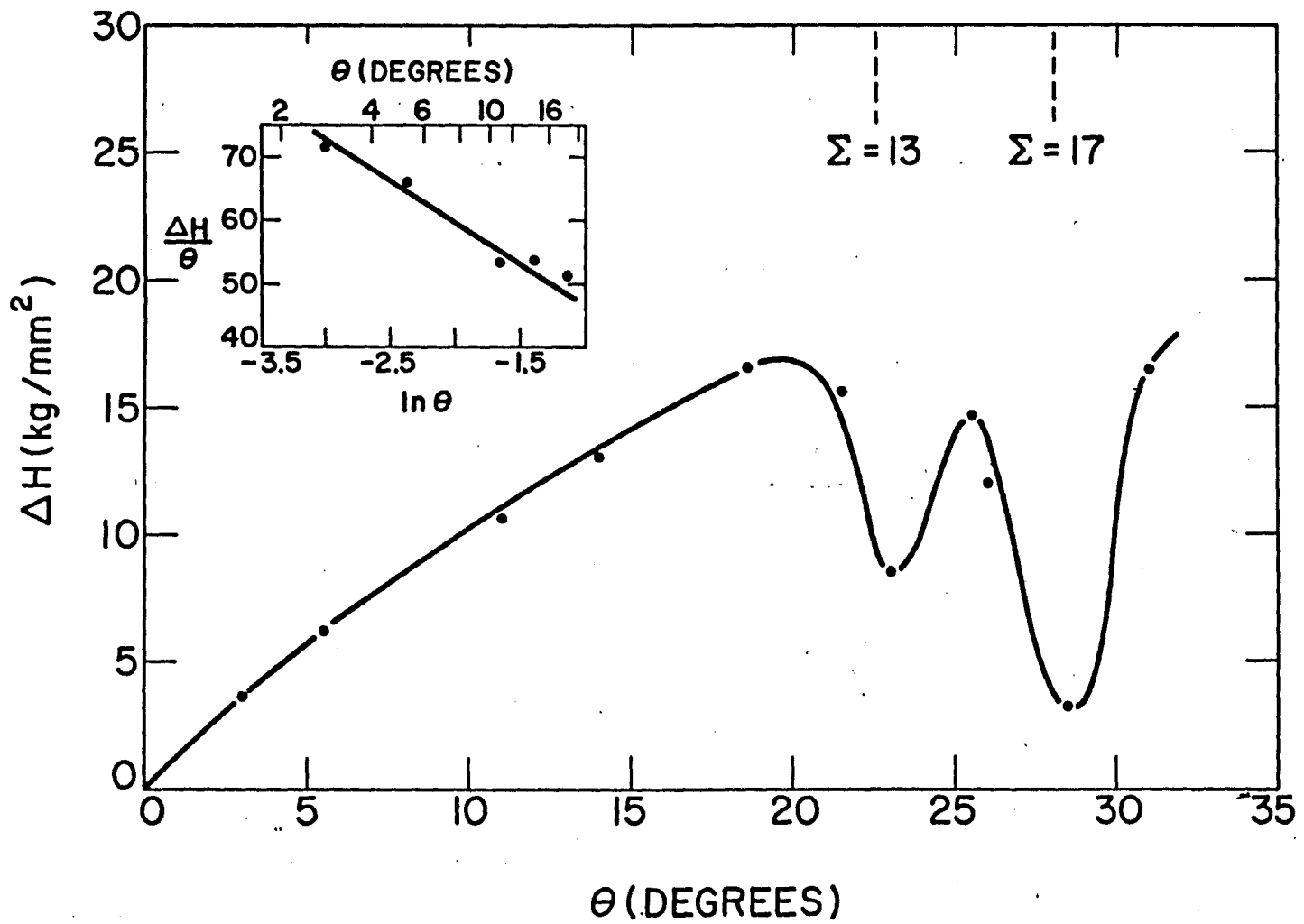Fig. 7. ΔH versus θ for different tilt axes. Misorientation vector along $[011]$.
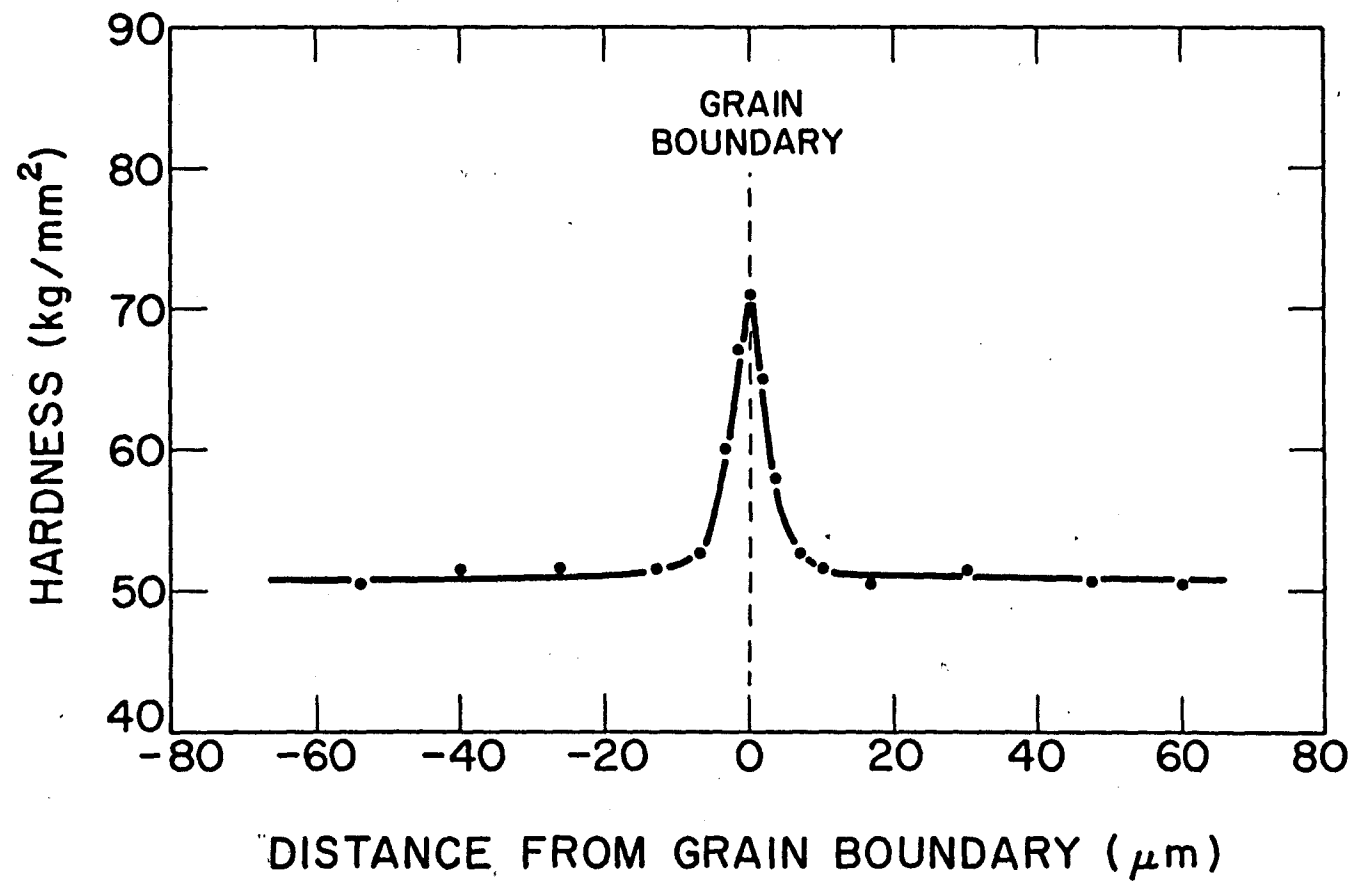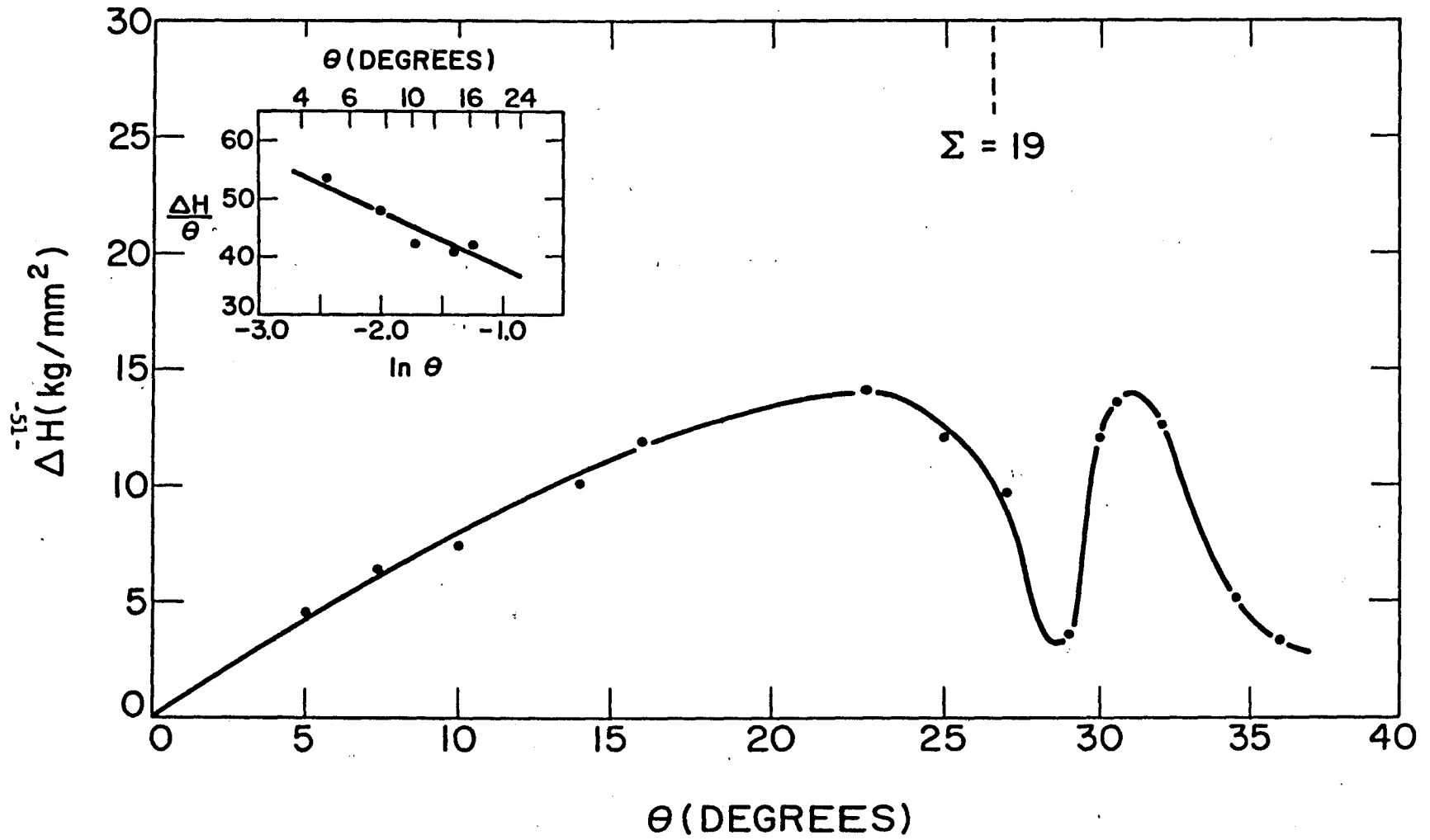
FIG. 1
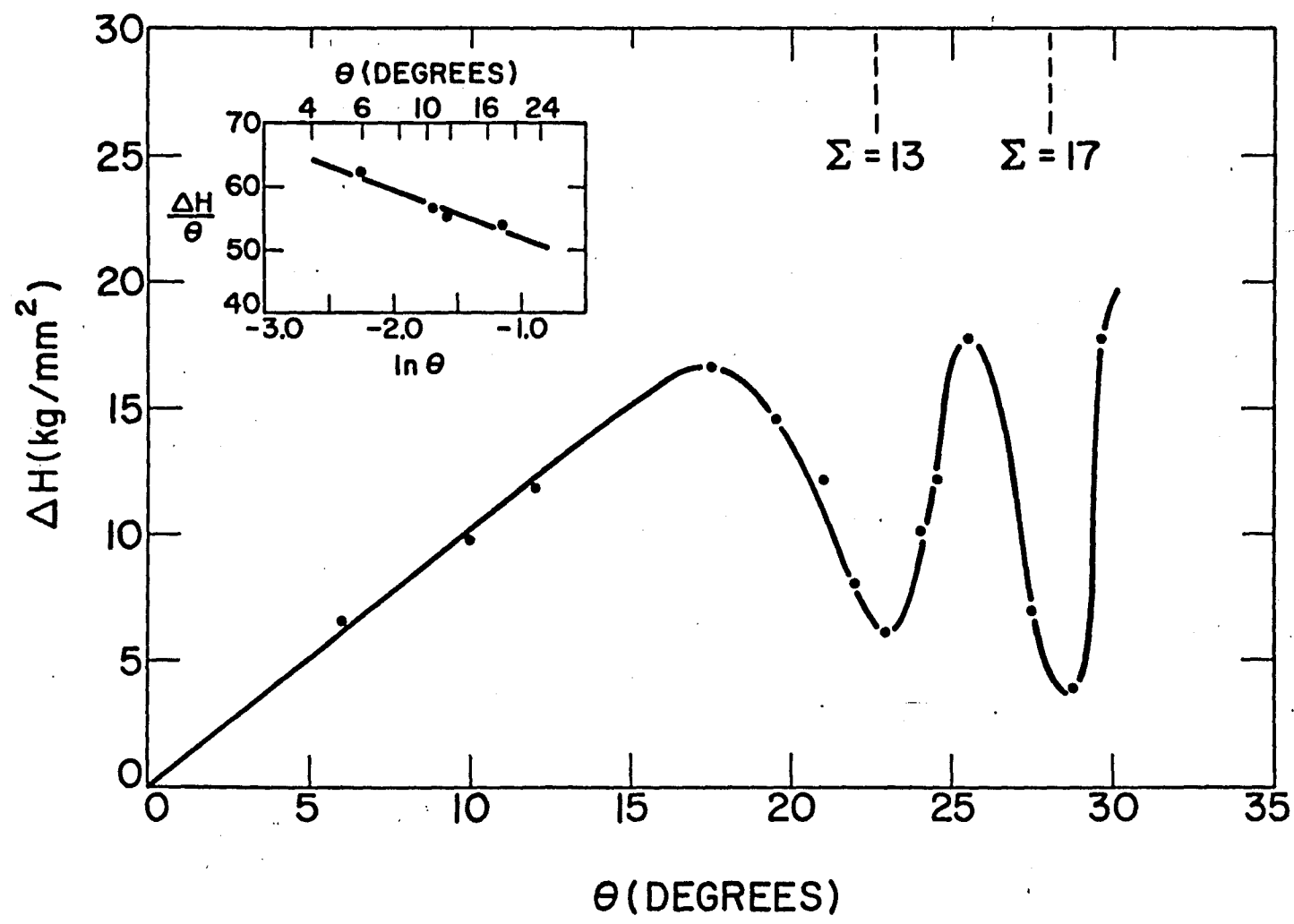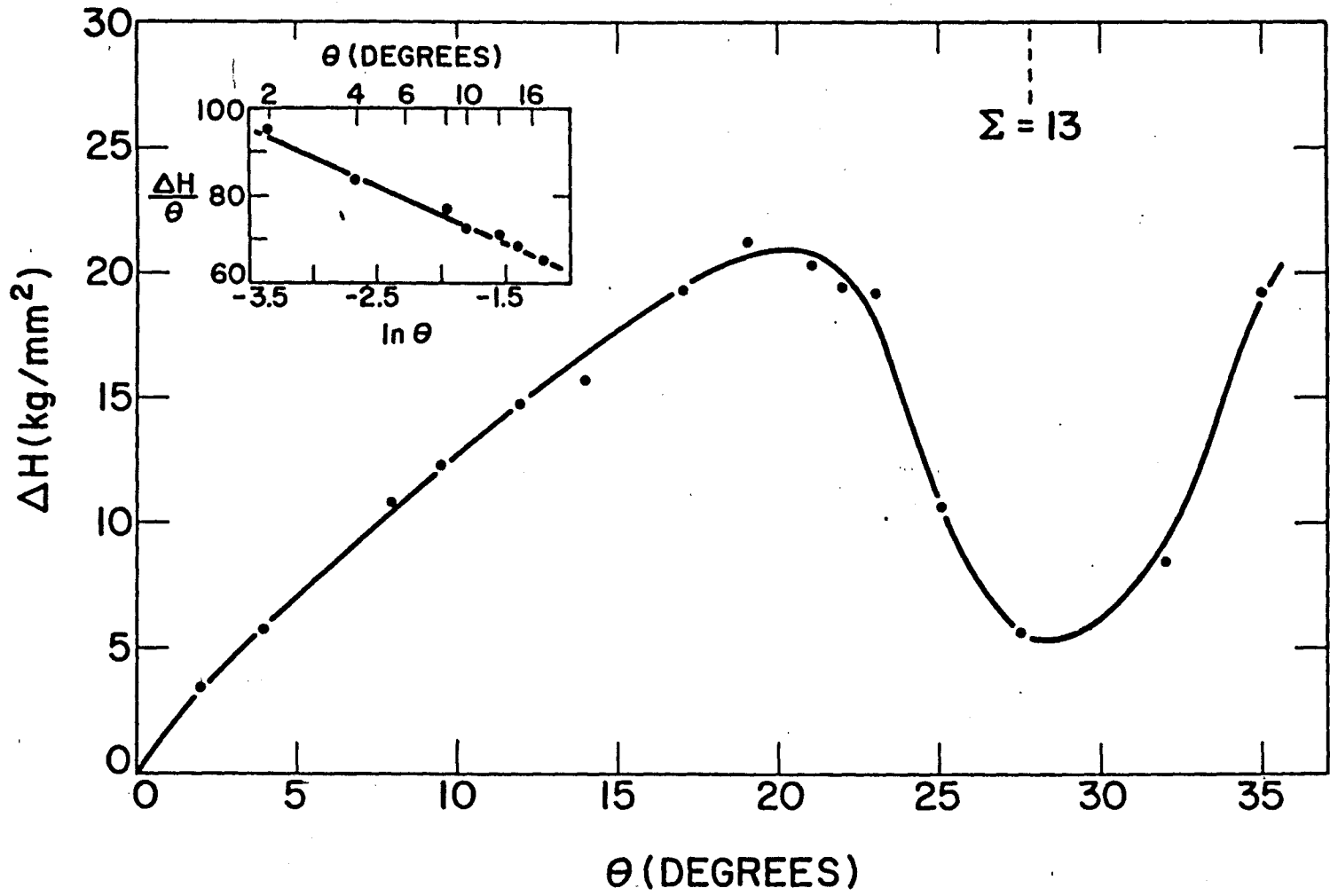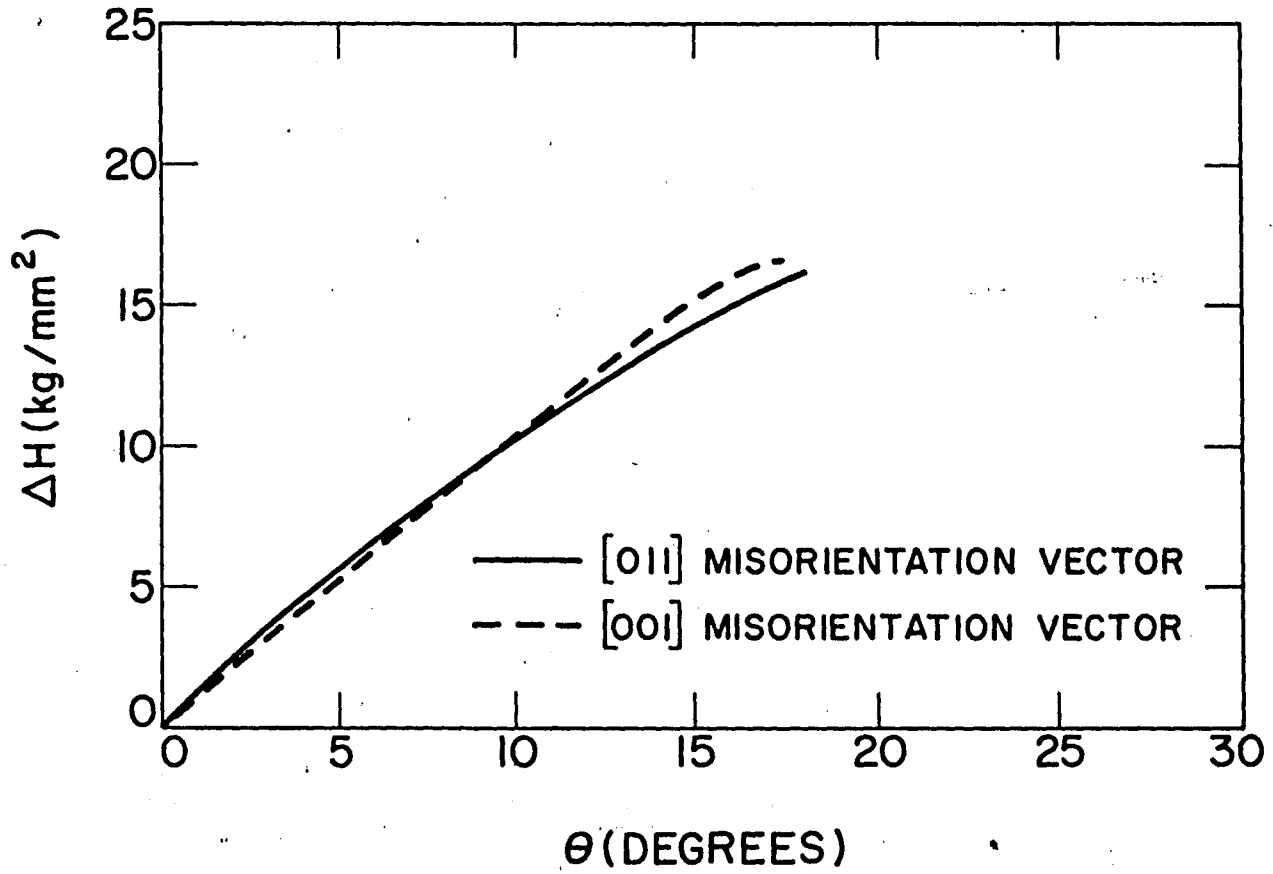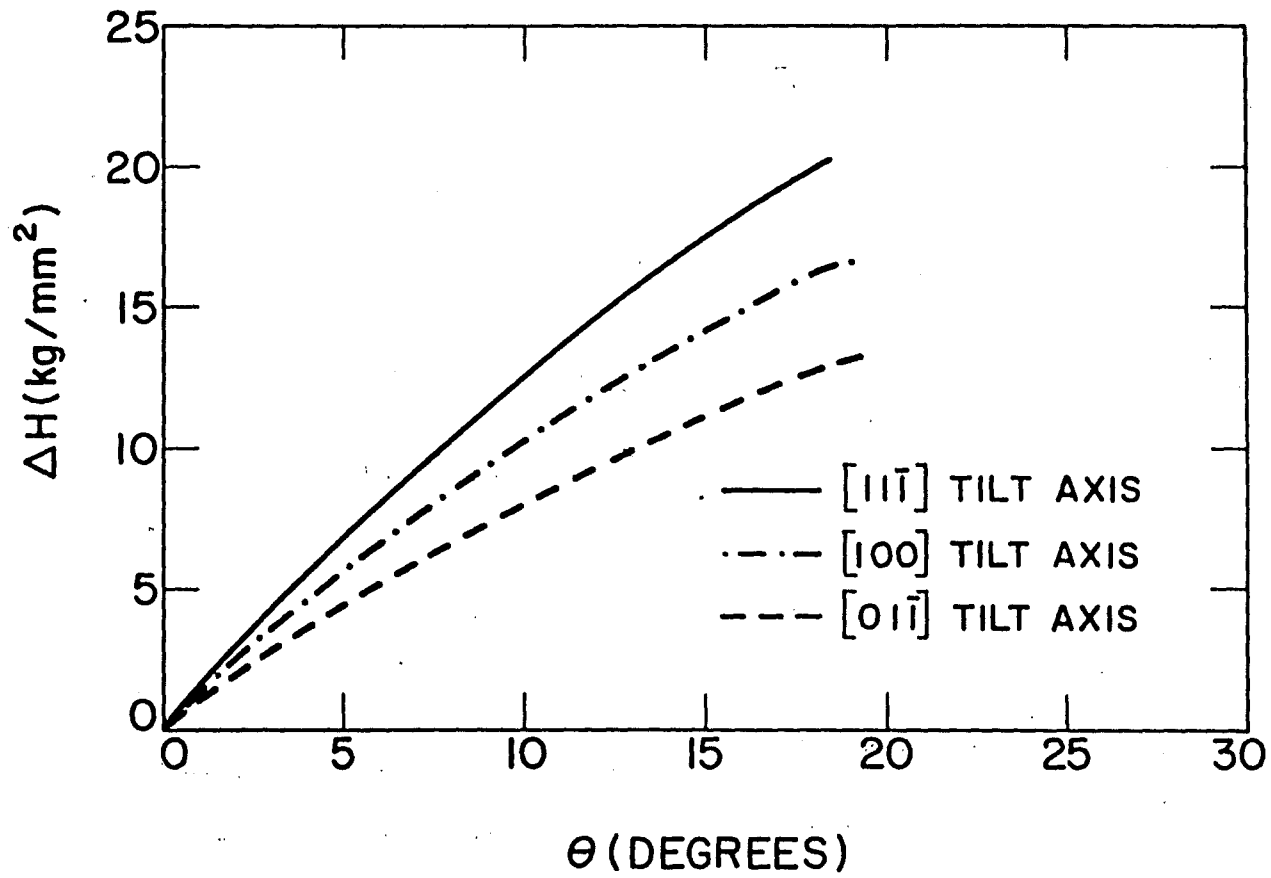
FIG. 2

FIG. 3

FIG. 4

FIG. 5

FIG. 6

FIG. 7

Vita

Bing-Chu Cai was born on September 12, 1938 in Shanghai, China. He was graduated from Chuan-Sha High School in Shanghai in 1957. In September 1957 he entered Shanghai Jiao-Tong University, Shanghai, China, earning a Bachelor of Science degree in the Department of Metallurgy and Materials Science in 1962. Subsequently, he joined the faculty of the Department of Metallurgy and Materials Science of Shanghai Jiao-Tong University and was promoted to Lecturer in 1978.

In August 1979, he entered the Department of Metallurgy and Materials Engineering, Lehigh University. He is a student member of the American Society for Metals.

In February 1967, Mr. Bing-Chu Cai was married to Xue-Ru Ding. He and his wife have two children.